국가기상위성센터
National Meteorological Satellite Center

SST (Sea Surface Temperature) Algorithm Theoretical Basis Document

(SST-v1.0)

NMSC/SCI/ATBD/SST, Issue 1, rev.0

2012.12.12

National Meteorological Satellite Center

REPORT SIGNATURE TABLE

Function	Name	Signature	Date
Prepared by			
Reviewed by			
Authorised by			

DOCUMENT CHANGE RECORD

Version	Date	Pages	Changes

Table of Contents

List of Tables

List of Figures

List of Acronyms

ARGO	Array for Real-time Geostrophic Oceanography
COMS	Communication, Ocean, and Meteorological Satellite
CTD	Conductivity, Temperature, and Depth
IR	Infrared
IOT	In-Orbit Test
JPL	Jet Propulsion Laboratory
MTSAT-1R	Multi-functional Transport Satellite 1 Replacement
NASA	National Aeronautics and Space Administration
NGSST	New Generation Sea Surface Temperature
NOAA	National Oceanic & Atmospheric Administration
MCSST	Multi-Channel Sea Surface Temperature
NESDIS	National Environmental Satellite, Data, and Information Service
OI	Optimum Interpolation
PFSST	PathFinder Sea Surface Temperature
RTM	Radiative Transfer Model
SST	Sea Surface Temperature
TIGR	TOVS Initial Guess Retrieval
TOVS	TIROS-N Operational Vertical Sounder

1. Overview

In order to understand and predict rapidly changing global climate, importance of ocean is being emphasized more than ever. To make more accurate weather forecast, not only numericcal weather prediction model of high performance computer, ocean-atmosphere data entered into the model are even more important. As the atmosphere is transformed by exchanging heat, water vapor, and momentum with ocean surface while passing over the sea, more accurate and precise high resolution ocean data are required. Among various ocean data, especially sea surface temperature (SST) is one of the most important variables which performs as a link between ocean and atmosphere. As COMS (Communication, Ocean and Meteorological Satellite) observes as often as every 15 minutes, SST field in significantly broader area can be obtained, which was not available to observe when it is covered by cloud. The frequent observation by geostationary satellite supplements the drawbacks of polar orbit satellites such as NOAA satellite and provides an opportunity to improve the accuracy of SST field. COMS SST adopts empirical regression algorithm and its coefficients in SST equation can be produced through comparing the thermal infrared channel radiances and actual sea observations and regression analysis. For the cloud screening, result of cloud detection algorithm previously done prior to SST calculation is used. Considering the possibility to fail in cloud processingwhich can produce abnormally high or low value in SST calculation, additional flag was given on its own. In the post process, a composite field is produced by averaging a certain period of calculated SST data. Following part of this document consists of theoretical background of SST algorithm, algorithm methodology, validation method, matchup criteria and validation result.

2. Background and Purpose

2.1. Physical Background and Limitation of SST Calculation Method

As SST is used for weather and climate monitoring, input data of numerical forecast model and for understanding various ocean phenomena, it is needed to be calculated with as highest accuracy as possible. To calculate SST from satellite data, coefficients can be calculated by comparing actual SST observations over the ocean or SST data from numeric model instead of them. Radiative transfer model (RTM) is performed with radiosonde measurements, simulated brightness temperature is determined using infrared channel response function of COMS MI(Meteorological Imager), then regression coefficients are determined using SST data used in the calculation of radiative transfer model.

Radiative transfer model ultimately calculates the skin temperature of sea surface, but the sea surface temperature largely differs depending on depth and time. Radiances measured by a satellite are from the sea surface at a few μm depth, and this is quite different from subsurface bulk temperature that is actually involved in the interaction between ocean-atmosphere according to time and other factors. The radiation emitted from sea surface is absorbed by thin cloud, water vapor, and fog as it passes the atmosphere, leading a different result from actual radiation from the sea. Therefore, to consider the atmospheric attenuation and temperature change depending on the depth of the sea, empirical Multi-Channel SST(MCSST) is commonly selected by comparing the sea bulk temperature with the brightness temperature difference of infrared channels, rather than depending on the radiative transfer model. As water temperature structure and atmosphere structure over the sea surface have diurnal variation, SST retrieval coefficients are produced for daytime and nighttime, separately.

Since Prabhakara et al.(1974) first suggested the Multi-Channel Sea Surface Temperature(MCSST) that can estimate the SST from infrared data observed from a satellite, many researchers such as McMillin(1975) and McClain(1985) began to calculate SST from satellite data. Then, Barton(1985) pointed out that sea surface radiation reached to the sensor of a satellite is affected by the path through which the atmosphere present between sea surface and a satellite, and he suggested the introduction of satellite zenith angle to calculation formula. Later on, the atmospheric correction formula in SST algorithm considering satellite zenith angle was equipped with the basic frame in NOAA/NESDIS Then, Walton(1988) and Walton et al.(1998) suggested non-linear SST algorithm (NLSST; Non-linear SST) and it is being used until today like the presented formula below. And, PFSST(Path Finder SST) method was suggested by NASA/JPL. This algorithm differentiates atmospheric water vapor load using the difference between the brightness temperature for the 11 and 12 ㎛ bands (Tb11-Tb12). Coefficients are determined for Tb11-Tb12 greater of less than 0.7K. In application, the coefficients and then weighted by measured Tb11-Tb12 (Brown and Minnett, 1999).

COMS SST algorithm is basically based on multi-channel regression analysis, and it is constructed to use the equation deducted by using COMS sensor response function (SRF) and radiative transfer model during the initial operation period of the satellite. This empirical algorithm greatly depends on the number and accuracy of collocation dataset used in the regression analysis. As many sea observations as possible is required to be collected, and when small number of data were used, the ocean characteristics could not be properly reflected. In particular, if the sea area of interest fluctuates seasonally, the accuracy of SST calculated can be improved only when at least 1 year's data is collected.

2.2. Purpose of Use

SST is the most basic variable of the ocean, and COMS can monitor near real time sea surface temperature condition at high resolution. Long term and short term variability of the SST can be grasped and ocean-atmosphere interaction can be better understood using the real time SST distribution. In particular, climate and global environment change monitoring as well as weather forecast is expected to be improved by assimilating these accurate and high resolution SSTs into the weather and climate models. It also helps to figure out the factors of frequent occurring severe weather, of which forecasting is hard, and to understand the interactions of ocean, atmosphere and land.

3. Algorithm

3.1. Theoretical Background

Since 1970's, NESDIS in USA has been producing and operating global scale SST. Before launching NOAA 7, SST algorithm was produced based only on 11㎛ brightness temperature. NOAA 9 had split window channels, but there is no 12 ㎛ channel in NOAA 10. Thus, 11 ㎛ single channel was used to make a rough calculation as belows:

$$ST \quad 1.1T_1 \qquad (1)$$

Later in 1981, NOAA 7 was launched. This satellite contains 11, 12, and 3.7 ㎛ channels. More accurate SST algorithm began to be developed using multi-channel measurement data. Prabhakara et al.(1974) first suggested Multi-Channel Sea Surface

Temperature(MCSST) algorithm that can estimate SST using satellite infrared channel data. Using this method, researchers like McMillin(1975)and McClain(1985) started to calculate SST from satellite data by following algorithm:

$$ST \quad T + \gamma(T_i - T_j) \qquad (2)$$

Here, $\gamma = k_i(k_i - k_j)$ is given and k_i, k_j are water vapor absorption coefficient.

Later Barton(1985) pointed out that radiation emitted from sea surface reached to the satellite sensor is affected by the path through the atmosphere it passes, and he suggested the introduction of satellite zenith angle consideration to SST calculation formula. Later on, the method was equipped with the basic frame in NOAA/NESDIS considering satellite zenith angle for adjusting atmosphere impact in SST calculation as belows:

$$SST = a + bT_i + c(T_i - T_j) + d(T_i - T_j)(\sec\theta - 1) \qquad (3)$$

When the atmosphere is very humid, value of γ is not a constant and SST may have larger error. Walton(1988) developed CPSST (Cross Product Sea Surface Temperature) algorithm as belows to resolve the problems due to the non-linearity of γ :

$$SST = \frac{SST_i - T_i}{SST_j - T_j + T_i^{\gamma*} + SST_i}(T_i - T_j) + T_j \qquad (4)$$

Here,

$$SST_i = A_i T_i + B_i,\ SST_j = A_j T_j + B_j,\ T_i^{\gamma*} = T_i + C$$

NLSST(Non-Linear Sea Surface Temperature) proposed by Walton et al(1998) is the one that supplemented the above algorithm further, expressed as belows:

$$NLSST = a + bT_i + cT_{sfc}(T_i - T_j) + d(T_i - T_j)(\sec\theta - 1) \qquad (5)$$

As surface temperature $_{fc}$ is not clearly known in this algorithm, it can be replaced with split window MCSST, or regularly forecasted model output data can be used. In current COMS algorithm, MCSST is employed as a basic method.

NASA/JPL developed and has used PFSST(Path Finder SST), in which different coefficients are induced depending on the water vapor content in atmosphere. PFSST algorithm is very similar to NLSST, but T_{11} T_{12} value of 0.7 is used for selecting coefficients in this algorithm, depending on the humidity of atmosphere.

$$PFSST = a_1 + b_1 T_i + c_1 T_{sfc}(T_i - T_j) + d_1 (T_i - T_j)(\sec\theta - 1)$$
$(T_{11} - T_{12} < 0.7)$
$$PFSST = a_2 + b_2 T_i + c_2 T_{sfc}(T_i - T_j) + d_2 (T_i - T_j)(\sec\theta - 1)$$
$(T_{11} - T_{12} \geq 0.7)$ (6)

Different coefficients in this algorithm are used for every month based on continuously updated sea-satellite match up database. For stable use of these regression coefficients, a certain amount of matchup database is required for a given period.

Stated on the user requirement, SST field should be produced not only for each image, but also for average of 1, 5, 10 days and 1 month. Various methods can be used to produce SST composite field, but simple averaging method and OI(Optimal Interpolation) are commonly used thesedays. First, the simplest way to determine the temporal average using the time series data of the given pixel can be expressed as belows:

$$SST(i,j) = \frac{1}{N} {}_{k=1} SST_k(i,j) \qquad (7)$$

Another way is to use 3-D OI with following related theoretical background: Measurement y can be expressed with observation model H and observation error n:

$$y = Hx + n \qquad (8)$$

Assuming that there is no correlation between observation error, and n:

$$< x \geqq < n \geqq < xn \quad \geqq 0 \qquad (9)$$

Covariance matrix of x and n can be expressed by $= < xx^T >$, $R = < nn^T >$, respectively. As OI is normally the determination process the solution of X satisfies the minimum of covariance, X can be determined that satisfied the condition that minimizes the diagonal element of following matrix P:

$$P = < (X - x)(X - x)^T > \qquad (10)$$

The solution of this formula is,

$$\begin{aligned} X &= PH^T R^{\ 1} y \\ P &= (S^{-1} + H^T R^{-1} H)^{-1} \end{aligned} \qquad (11)$$

This can be expressed in another way like this:

$$\begin{aligned} X &= SH^T (HSH^T + R)^{-1} y \\ P &= S - SH^T (HSH^T + R)^{-1} HS \end{aligned} \qquad (12)$$

Or, X that satisfies following formula is the same answer:

$$J = X^T S^{-1} x + n^T R^{-1} n \qquad (13)$$

Error can be objectively minimized by this OI method, but a significant amount of computing resources is needed for matrix inversion and calculation. Also, the temperature field produced here can be significantly smoothed depending on the temporal and spatial scales of phenomena during the calculation process. Matrix X in above formula was determined and used as SST temporal and spatial composite field.

Formula (12) by the method of Bretherton et al.(1976)can be expressed as follows. A in formula (14) is the autocorrelation matrix of observation state vector, and   is calculated in formula (15).

$$X \quad CA \;\, ^{1}y \qquad (14)$$

$$C(r) = (1 - r^2)\exp(-r^2/2) \qquad (15)$$
$$r^2 = (\frac{\Delta d_x}{L_x})^2 + (\frac{\Delta d_y}{L_y})^2 + (\frac{\Delta d_t}{L_t})^2$$

Here d_x and d_y indicate the distances from east to west and from north to south, respectively, and t denotes time. When OI method is used in the data around the corresponding pixel to composite, certain time interval L_t and spatial length scale L_x, L_y should be set up. Each scale corresponds to the length scale of ocean phenomenon in each direction (decorrelation scale). The composite field can be produced through sequentially moving the temporal and spatial window within the whole North Pacific area with constant 180km spatial length scales for each east-west and north-south direction.

3.2. Methodology

Coefficients in SST equation are obtained through empirical regression analysis using the match up data between ocean surface and satellite observations. Algorithms used here are shown in Table 1. T3, T4, and T5 indicate the brightness temperature of COMS channels, SWIR3.75㎛, IR10.8㎛, and IR12.0㎛. For the clear pixels from cloud detection output, brightness temperatures of COMS channel 2(SWIR 3.75㎛), channel 4(IR10.8㎛), and channel 5(IR12.0㎛), and previously prepared SST coefficients are used to retreive SSTs as shown in Table 1. Various SST algorithm coefficients were readily prepared considering the contingency situation such as any possible loss of channel data. For example, if there is a problem in 3.7㎛ channel data, neither dual nor triple window method cannot be used. The current default method is set to split window MCSST (MCSST45). In the case of MTSAT-1R, SST regression coefficients were updated every day in the early operation period via matchup between satellite and numerical prediction model data. NASA/JPL Pathfinder uses PFSST algorithm, which applies different SST coefficients based on 0.7℃ of IR channel difference. This method is not applied real time, but the coefficient is made by collecting data for a month after data reception. Coefficients has updated every month according to the list of PFSST product. For the COMS SST algorithm, coefficients of each equation are determined by regression analysis using the satellite and ocean surface collocation dataset during the IOT period, Then, these coefficients are used for the calculation of SST.

Table 1. SST equation formula used for the derivation of regression coefficients. The temperatures T3, T4, T5 are the brightness temperatures of channels 3.75㎛, 10.8㎛, and 12.0㎛, respectively.

Method	Window	Formular	Condition
Single channel SST without satellite zenith angle correction	single channel	SST3 = C1*T3 + C2	-
		SST4 = C1*T4 +C2	-
		SST5 = C1*T5 + C2	-
Multi-channel SST without satellite zenith angle correction	dual	SST34 = C1*T4 + C2*(T3-T4) + C3	-
	split	SST45 = C1*T4 + C2*(T4-T5) + C3	-
	triple	SST345 = C1*T4 + C2*(T3-T5) + C3	-
Multi-channel SST with satellite zenith angle correction	dual	MCSST34 = C1*T4 + C2*(T3-T4) + C3*(T3-T4)*(secsza-1) + C4	-
	split	MCSST45 = C1*T4 + C2*(T4-T5) + C3*(T4-T5)*(secsza-1) + C4	-
	triple	MCSST345 = C1*T4 + C2*(T3-T5) + C3*(T3-T5)*(secsza-1) + C4	-
Multi-channel Non-linear SST	dual	NLSST34 = C1*T4 + C2*MCSST45*(T3-T4) + C3*(secsza-1) + C4	-
	split	NLSST45 = C1*T4 + C2*MCSST45*(T4-T5) + C3*(T4-T5)*(secsza-1) + C4	-
	triple	NLSST345 = C1*T4 + C2*MCSST45*(T3-T5) + C3*(secsza-1) + C4	-
PFSST (PathFinder SST)	split	PFSST1 = C11*T4 + C12*MCSST45*(T4-T5) + C13*(T4-T5)*(secsza-1) + C14	T4-T5<0.7
		PFSST2 = C21*T4 + C22*MCSST45*(T4-T5) + C23*(T4-T5)*(secsza-1) + C24	T4-T5>0.7

3.3. Retrieval Process

3.3.1. Overviews of the Retrieval Process

COMS algorithm consists of 3 steps(Figure 1). The first step is pre-processing which generates matchup database using temporal and spatial collocation procedure between satellite and ocean surface observations. By using the matchup database, SST retrieval coefficients are derived via multivariate regression analysis. This pre-processing is conducted off line. Real-time processing is the second step, which calculate SST values applying the regression coefficients to the SST equations (mainly MCSST method) and using the COMS channels brightness temperatures and satellite zenith angle information for the corresponding pixels. After that daily, 5-day, 10-day and monthly composite SSTs are generated every day in the post-process. In application, three phases can be considered for SST coefficients determination, which are IOT phase, post-IOT phase and stable phase. At the early of COMS operation, the coefficients from the actual match up database cannot be prepared. Thus, during the IOT phase, theoretically derived coefficients are used for SST calculation. These coefficients can be generated by RTM simulation study. For the RTM simulation, atmospheric temperature and humidity vertical structure data is required as an input. In this COMS simulation study, MODTRAN5 radiative transfer model and TIGR profiles are utilized. In addition, COMS sensor response function(SRF) is also used for generation of COMS theoretical SST coefficients. To determine the SST regression coefficients for the post-IOT phase, match up database between the COMS and conventional SST measurements needs to be acquired during the IOT period. After IOT period, when COMS starts to operate officially, SST is calculated real time using the coefficient induced using the match up database acquired during IOT. For the stable phase SST retrieval, the regression coefficients can be updated every 6 month or 1 year by using larger number of matchup datasets, and through this, the accuracy of generated SST values are expected to be improved.

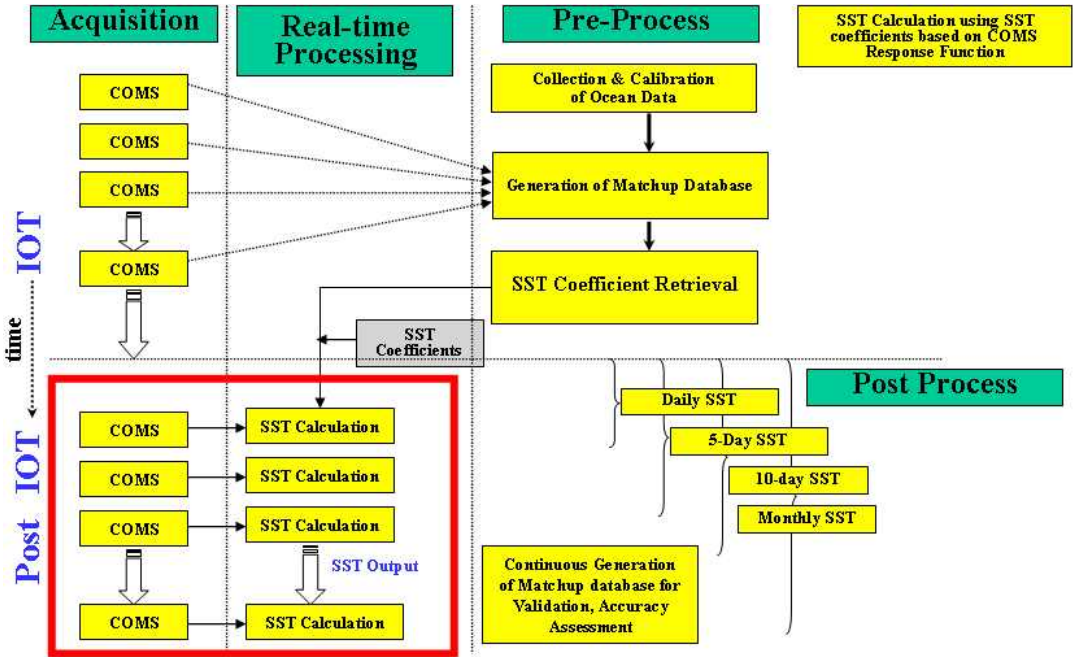

Fig. 1. Conceptual diagram for SST estimation process.

COMS SST algorithm employs 13 different SST retrieval methods (or equations) as shown in Table 1. It is composed so that users can select an algorithm among their results according to convenience and demand of user. The current default algorithm is split window MCSST, but problem of each channel data can occur after satellite launching. To cope with this situation, coefficients needed in other algorithms were produced and provided as well, so that the user can make choice.

3.3.2. Matchup Data

Coefficients required to calculate SST is derived using actual ocean surface observation data and the brightness temperatures in infrared area by empirical regression analysis, A large amount of well selected conventional SST observation data is needed. SST data observed from satellite tracking drift buoy, ARGO float, and CTD are representative, and moored buoy data is also available for the coast area.

To determine SST coefficient, first, collocation match up database of actually observed SST data and COMS satellite data SST observation data should include time and location (latitude, longitude) information, SST temperature and observation depth. To understand the characteristics of error in observed SST, data related to atmosphere condition should be saved, as well. Depending on the observation type, as buoy includes additional information on atmosphere temperature or sea surface wind, various factors affecting error can be grasped.

As for SST data collectable real time, there is drift buoy data communicated via GTS(Global Telecommunication System) network in Korea Meteorological Administration. As this data is being operated systematically real time so far, it seems that data can be supplied stably without any problem.

As COMS has not been launched yet, data from MTSAT-1R, the most similar to COMS satellite, was used to make collocation database exemplary. Maximum time window between buoy-satellite data was given as 30 minutes, and spatial window was 5 km considering the ground resolution of the satellite. Following these collocation criteria, match up database was made using the data shown in Table 2. When it is operated real time, it is structured so that matched data is automatically added to xisting database.

Table 2. Information of collocation database on area, period, data numbers over the East Asian region

Matchup Database	**Area**	**Period**	**# of matchups Day**	**# of matchups Night**
MTSAT-1R - GTS Drifter	10°S ~ 60°N 80°E ~ 180°E	2005.7 ~ 2006.6	19540	72451

In match up database, year, month, day, hour, minute of buoy observation time, latitude and longitude of COMS satellite observation pixel location, averaged satellite values within collocation window (solar zenith angle, satellite zenith angle, 5 channel data), minimum, maximum and standard deviation of 5 channels in 3x3 pixel area latitude and longitude of buoy observation location, buoy ID, buoy SST, observation depth, SST guess derived from RTM simulated coefficients, wind direction, wind velocity, and air temperature from buoy observation and COMS observation time information are documented in order. These matchup data are used to calculate the coefficient of SST formula and used as basic data to evaluate the accuracy of calculated SST. When MTSAT-1R data and GTS drifter data were collected from July 2005 to June 2006, 19,540 data for daytime and 72,451 data for nighttime were obtained. The locations of the collocation points for this period are seen in Figure 3.

Table 3. Information of collocation database on area, period, data numbers for the full disk region

Matchup Database	**Area**	**Period**	**# of matchups Day**	**# of matchups Night**
MTSAT-1R - GTS Drifter	60°S ~ 60°N 80°E ~ 180°E	2007.9 ~ 2008.6	6,182	93,536

Besides COMS satellite data, cloud mask, land/sea mask, and satellite zenith angle are needed. Normally, daytime or nighttime condition is determined by if the solar zenith angle is higher or lower than the given value (<80°) at each pixel, and daytime or nighttime coefficients are used accordingly. In this case, different coefficients for daytime or nighttime are applied for one COMS observation time image data, in order not to make a spatial discotinuity in the middle of the SST image ultimately calculated. In this case, It looks like that a long north-to-south SST frontal zone is abnormally distributed over the ocean, which is not suitable for real situation and for the input of numerical prediction model. This rapid spatial SST discontinuity may cause instability on the boundary layer of the ocean-atmosphere coupled model. Over the ocean, as stratification does not completely developed within 2 to 3 hours after sunrise, each of daytime or nighttime coefficients can be used to calculate SST over the one COMS Full Disk area at the transition period. Error due to this prescription is inevitable, but its impact is considered to be not so much as the problem due to discontinuous line. Therefore, daytime and nighttime coefficients application is divided based on the reception time of the satellite.

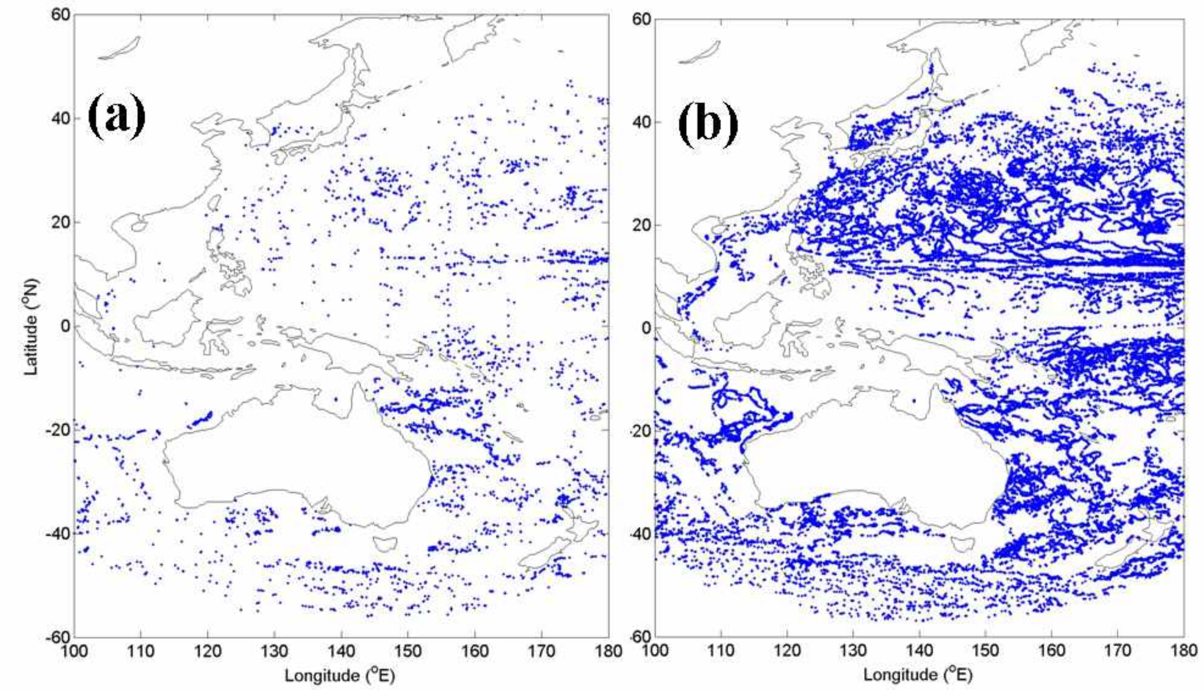

Fig. 3. Location of collocation data points between MTSAT-1R data and GTS drifter data for the daytime and nighttime MTSAT-1R passes over the full disk region.

Match up database was produced using the MTSAT-1R data for full disk domain for 9 months from September 2007 to July 2008 through collocation with buoy data. As shown in Table 3, the number of gathered daytime and nighttime match up datasets are 6,182 and 93,536, respectively, Fig. 3 shows the locations of all match up points obtained for global domain. The larger number of data produced at nighttime is thought to be caused from weaker cloud screening at night when solar channel data can not be used for cloud detection.

3.3.3. Cloud Screening

To remove pixels contaminated by cloud in the obtained match up data, further cloud screening procedure is employed in this study. Additional cloud masking methods that applied are summarized in Table 4 and Table 5. To remove non-ideal cases, limit range was given for the estimate of SST calculated using COMS channel response function. Pixels largely underestimated were also removed through comparison with climate sea surface temperature field.

To remove pixels contaminated by cirrus, thin cirrus dynamic threshold test process was employed as shown in Figure 4. A thin cirrus test threshold value was given to the brightness temperature different between channel 4 and 5, but not a constant value is used, but a dynamic threshold varying from 1℃ to 6℃ was applied regarding channel 4 brightness temperature. The thresholds are calculated by Formula (16). If the temperature of channel 4 is higher than 20℃, the threshold value is constantly set to 6℃.

$$ch45\_diff\_threshold = 0.0032*(Tir1)^2+0.0996*Tir1+1.6071 \qquad (16)$$

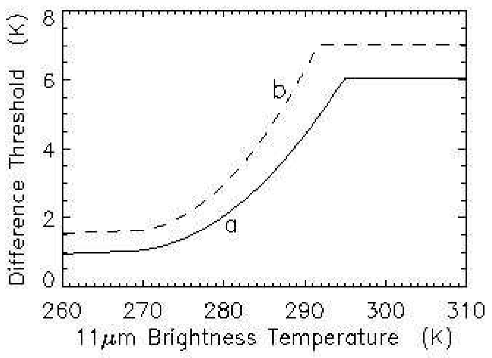

Fig. 4. Threshold for the 11-12μm test as a function of the 11μm BT. Curve a) is for the nadir view within 50 km of the sub-satellite track, and curve b) the same for the corresponding forward view.

Table 4. Tests for eliminating cloudy or partly-cloudy pixel of daytime COMS data.

Test ID	Description	Clear Condition
1	IIs reflectivity of channel 1 smaller than 6%?	<6
2	Is standard deviation of channel 1 reflectivity in 3×3 pixel area smaller than 0.5%?	<0.5℃
3	Standard deviation of channel 4 brightness temperature in 3×3 pixel area is smaller than 1℃?	<1℃
4	Standard deviation of channel 5 brightness temperature in 3×3 pixel area is smaller than 1℃?	<1℃
5	Is satellite zenith angle smaller than 65 degree?	<65
6	Channel 4 brightness temperature of regarding pixel is larger than -3℃?	>-3℃
7	Channel 5 brightness temperature of regarding pixel is larger than -3.5℃?	>-3.5℃
8	The difference of maximum and minimum channel 1 reflectivity in 3×3 area is smaller than 3%?	<3
9	The difference of maximum and minimum channel 4 brightness temperature in 3x3 pixel area is smaller than 3℃?	<3℃
10	The difference of maximum and minimum channel 5 brightness temperature in 3x3 pixel area is smaller than 3℃?	<3℃
11	Is the brightness temperature difference between channel 4 and 5 larger than 0℃ and smaller than 6℃ ?	0℃< <6℃
12	Is the collocated buoy SST larger than –2℃ and smaller than 35℃?	-2℃< <35℃
13	Is the difference between SST_guess calculated using the coefficient derived from RTM simulation and collocated buoy observation larger than -4℃ ?	>-4℃
14	Is the difference between buoy observed SST and the climate SST smaller than 3℃ ?	<3℃
15	Is the difference between SST_guess and the climate SST larger than -4℃ ?	>-4℃
16	IIs the brightness temperature difference between channel 4 and 5 smaller than dynamic cirrus test threshold?	< dynamic threshold

Table 5. Tests for eliminating cloudy or partly-cloudy pixels of nighttime COMS data

Test ID	Description	Clear Condition
1	Is standard deviation of channel 4 brightness temperature in 3x3 pixel area smaller than 1℃?	<1℃
2	Is standard deviation of channel 5 brightness temperature in 3x3 pixel area smaller than 1℃?	<1℃
3	Is satellite zenith angle smaller than 65 ?	<65
4	Is channel 4 brightness temperature of regarding pixel larger than -3℃ ?	>-3℃
5	Is channel 5 brightness temperature of regarding pixel larger than -3.5℃ ?	>-3.5℃
6	The difference of maximum and minimum channel 4 brightness temperature in 3x3 pixel area is smaller than 3℃?	<3℃
7	The difference of maximum and minimum channel 5 brightness temperature in 3x3 pixel area is smaller than 3℃?	<3℃
8	Is the brightness temperature difference between channel 4 and 5 larger than 0℃ and smaller than 6℃ ?	0℃< <6℃
9	Is the collocated buoy SST larger than –2℃ and smaller than 35℃?	-2℃< <35℃
10	Is the difference between SST_guess calculated using the coefficient derived from RTM simulation and collocated buoy observation larger than -4℃ ?	>-4℃
11	Is the difference between buoy observed SST and the climate SST smaller than 3℃ ?	<3℃
12	Is the difference between SST_guess and the climate SST larger than -4℃ ?	>-4℃
13	Is the brightness temperature difference between channel 4 and 5 smaller than dynamic cirrus test threshold?	< dynamic threshold

3.3.4. STT Coefficient Generation

The collocated data to determine the SST regression coefficients are satellite level1B channel data (VIS0.65㎛, SWIR3.75㎛, IR10.8㎛, IR12.0㎛) and buoy observation data. Buoy observation data should include observation time information, location (latitude, longitude), SST and observation depth. By comparing these information with COMS satellite data, it is checked if buoy data and satellite data are within the given time window(30 minutes) and within the given distance (5 km). Cloud cleared collocated data are saved. This collocation data can be produced during the initial operation period after satellite launch. Using the cloud screened and quality controlled matchup dataset, SST retrieval coefficients can be generated through regression analysis. For the COMS SST retrieval, different coefficients are applied for daytime and nighttime. Day or night condition is determined based on the satellite observation time, Cloud screening and quality control are conducted to the match up data as discussed previouslyand the coefficients to be used in each algorithm for each daytime and nighttime case are obtained through a series of empirical regression analysis. Table 6 and 7 show the SST retrieval algorithm coefficients by MTSAT-1R Collocation data for East Asian region.

SST equations and the coefficients for daytime and nighttime in global (full disk) domain are shown in Table 8 and Table 9, respectively. Split Window MCSST regression result has 0.92℃ and 0.94℃ RMS error in daytime and nighttime case, respectively.

Table 6. Daytime SST Coefficients for MTSAT-1R data over the East Asian Seas

```
================= Daytime SST Coefficients & Regression Errors ================
I. Single channel SST without satellite zenith angle correction
   SST3 = C1*T3 + C2 , SST4 = C1*T4 +C2 , SST5 = C1*T5 + C2
II. Multi channel SST without satellite zenith angle correction
   Dual   : SST34     C1*T4 + C2*(T3-T4) + C3
   Split  : SST45     C1*T4 + C2*(T4-T5) + C3
   Triple : SST345    C1*T4 + C2*(T3-T5) + C3
III. Multi-channel SST with satellite zenith angle correction ------------------
   Dual   : MCSST34     C1*T4 + C2*(T3-T4) + C3*(T3-T4)*(secsza-1) + C4
   Split  : MCSST45     C1*T4 + C2*(T4-T5) + C3*(T4-T5)*(secsza-1) + C4
   Triple : MCSST345    C1*T4 + C2*(T3-T5) + C3*(T3-T5)*(secsza-1) + C4
IV. Non-linear SST  -------------------------------------------------------------
   Dual   : NLSST34  = C1*T4 + C2*MCSST45*(T3 T4) + C3*(secsza 1) + C4
   Split  : NLSST45  = C1*T4 + C2*MCSST45*(T4 T5) + C3*(T4 T5)*(secsza 1) + C4
   Triple : NLSST345 = C1*T4 + C2*MCSST45*(T3 T5) + C3*(secsza 1) + C4
V. PFSST
   T4-T5<0.7 : PFSST1    C1*T4 + C2*MCSST45*(T4-T5) + C3*(T4-T5)*(secsza-1) + C4
   T4-T5>0.7 : PFSST2    C1*T4 + C2*MCSST45*(T4-T5) + C3*(T4-T5)*(secsza-1) + C4
--------------------------------------------------------------------------------
```

Algorithm :	C1	C2	C3	C4	RMS	Bias
SST3 :	0	0	0	0	0	0
SST4 :	1.101010	3.267147	0	0	1.471338	0.000220
SST5 :	1.102342	4.604476	0	0	1.990979	0.000144
SST34 :	0	0	0	0	0	0
SST45 :	1.115510	0.410952	3.505930	0	1.655351	0.000219
SST345 :	0	0	0	0	0	0
MCSST34 :	0	0	0	0	0	0
MCSST45 :	1.037155	2.118685	0.457718	1.684577	0.847684	0.000218
MCSST345:	0	0	0	0	0	0
NLSST34 :	0	0	0	0	0	0
NLSST45 :	0.978148	0.073093	0.819438	3.017323	0.839714	0.000218
NLSST345:	0	0	0	0	0	0
PFSST1 :	1.032548	0.033559	2.798520	2.265775	0	0
PFSST2 :	0.967750	0.075641	0.744650	3.142197	0.834190	-0.000003

Table 7. Nighttime SST Coefficients for MTSAT-1R data over the East Asian Seas

```
                    Daytime SST Coefficients & Regression Errors
I. Single channel SST without satellite zenith angle correction ----------------
   SST3   C1*T3 + C2 , SST4   C1*T4 +C2 , SST5   C1*T5 + C2
II. Multi-channel SST without satellite zenith angle correction ----------------
   Dual   : SST34    C1*T4 + C2*(T3-T4) + C3
   Split  : SST45  = C1*T4 + C2*(T4-T5) + C3
   Triple : SST345 = C1*T4 + C2*(T3-T5) + C3
III. Multi-channel SST with satellite zenith angle correction
   Dual   : MCSST34  = C1*T4 + C2*(T3-T4) + C3*(T3-T4)*(secsza-1) + C4
   Split  : MCSST45  = C1*T4 + C2*(T4-T5) + C3*(T4-T5)*(secsza-1) + C4
   Triple : MCSST345   C1*T4 + C2*(T3-T5) + C3*(T3-T5)*(secsza-1) + C4
IV. Non-linear SST  ------------------------------------------------------------
   Dual   : NLSST34    C1*T4 + C2*MCSST45*(T3-T4) + C3*(secsza-1) + C4
   Split  : NLSST45    C1*T4 + C2*MCSST45*(T4-T5) + C3*(T4-T5)*(secsza-1) + C4
   Triple : NLSST345   C1*T4 + C2*MCSST45*(T3-T5) + C3*(secsza-1) + C4
V. PFSST  ----------------------------------------------------------------------
   T4-T5<0.7 : PFSST1   C1*T4 + C2*MCSST45*(T4-T5) + C3*(T4-T5)*(secsza-1) + C4
   T4-T5>0.7 : PFSST2   C1*T4 + C2*MCSST45*(T4-T5) + C3*(T4-T5)*(secsza-1) + C4
```

Algorithm :	C1	C2	C3	C4	RMS	Bias
SST3 :	0.618372	13.834317	0	0	3.004241	0.000171
SST4 :	1.109305	3.566514	0	0	1.431108	0.000281
SST5 :	1.119503	5.014503	0	0	1.917330	-0.000265
SST34 :	1.242919	-0.510877	0.204503	0	3.037746	-0.000297
SST45 :	1.120677	-0.258814	3.731531	0	1.535777	-0.000281
SST345 :	1.499304	-1.276618	-4.021108	0	6.542086	-0.000342
MCSST34 :	1.103189	0.190857	-0.251158	3.812083	1.310965	-0.000280
MCSST45 :	1.025495	2.105861	0.317668	1.950496	0.898502	-0.000286
MCSST345:	1.082864	0.198658	-0.233103	4.010041	1.272329	-0.000274
NLSST34 :	1.140475	0.005283	1.440987	2.780641	1.317590	-0.000290
NLSST45 :	0.962003	0.071604	0.695688	3.415856	0.904371	0.000257
NLSST345:	1.128961	0.005973	1.574879	2.761372	1.265849	0.000284
PFSST1 :	1.018411	0.033853	2.067455	2.606112	0	0
PFSST2 :	0.000000	0.000000	0.000000	0.000000	0.000000	0.000000

Table 8. Daytime SST Coefficients for MTSAT-1R data over the full disk region

```
                    Daytime SST Coefficients & Regression Errors
I. Single channel SST without satellite zenith angle correction ----------------
        SST3 C1*T3 + C2 ,SST4 C1*T4 +C2 ,SST5 C1*T5 + C2
II. Multi channel SST without satellite zenith angle correction
   Dual   : SST34  C1*T4 + C2*(T3-T4) + C3
   Split  : SST45 =C1*T4 + C2*(T4 T5) + C3
   Triple : SST345 C1*T4 + C2*(T3-T5) + C3
III. Multi channel SST with satellite zenith angle correction
   Dual   : MCSST34  C1*T4 + C2*(T3-T4) + C3*(T3-T4)*(secsza-1) + C4
   Split  : MCSST45  C1*T4 + C2*(T4-T5) + C3*(T4-T5)*(secsza-1) + C4
   Triple : MCSST345 C1*T4 + C2*(T3-T5) + C3*(T3-T5)*(secsza-1) + C4
IV. Non-linear SST  ------------------------------------------------------------
   Dual   : NLSST34  C1*T4 + C2*MCSST45*(T3-T4) + C3*(secsza-1) + C4
   Split  : NLSST45  C1*T4 + C2*MCSST45*(T4-T5) + C3*(T4-T5)*(secsza-1) + C4
   Triple : NLSST345 C1*T4 + C2*MCSST45*(T3-T5) + C3*(secsza-1) + C4
V. PFSST  ----------------------------------------------------------------------
   T4 T5<0.7 : PFSST1=C1*T4 + C2*MCSST45*(T4 T5) + C3*(T4 T5)*(secsza 1) + C4
   T4-T5>0.7 : PFSST2 C1*T4 + C2*MCSST45*(T4-T5) + C3*(T4-T5)*(secsza-1) + C4
```

Algorithm :	C1	C2	C3	C4	RMS	Bias
SST3 :	0	0	0	0	0	0
SST4 :	1.118537	4.373433	0	0	2.211642	0.000093
SST5 :	1.087934	6.759830	0	0	3.027127	-0.000031
SST34 :	0	0	0	0	0	0
SST45 :	1.142775	-0.524149	4.829164	0	2.583136	0.000103
SST345 :	0	0	0	0	0	0
MCSST34 :	0	0	0	0	0	0
MCSST45 :	1.039460	2.254069	0.827841	1.356577	0.920695	0.000084
MCSST345:	0	0	0	0	0	0
NLSST34 :	0	0	0	0	0	0
NLSST45 :	0.962569	0.073570	0.846559	3.280368	0.929144	0.000072
NLSST345:	0	0	0	0	0	0
PFSST1 :	1.015200	0.028266	2.588066	2.367115	0	0
PFSST2 :	0.953931	0.075317	0.829028	3.347202	0.919693	0.000069
NLSST345:	1.128961	0.005973	1.574879	2.761372	1.265849	0.000284
PFSST1 :	1.018411	0.033853	2.067455	2.606112	0	0
PFSST2 :	0.000000	0.000000	0.000000	0.000000	0.000000	0.000000

Table 9. Nighttime SST Coefficients for MTSAT-1R data over the full disk region

```
================= Daytime SST Coefficients & Regression Errors ================
I. Single channel SST without satellite zenith angle correction ----------------
   SST3   C1*T3 + C2 , SST4   C1*T4 +C2 , SST5   C1*T5 + C2
II. Multi-channel SST without satellite zenith angle correction ----------------
   Dual   : SST34    C1*T4 + C2*(T3-T4) + C3
   Split  : SST45    C1*T4 + C2*(T4-T5) + C3
   Triple : SST345 = C1*T4 + C2*(T3 T5) + C3
III. Multi-channel SST with satellite zenith angle correction ------------------
   Dual   : MCSST34  = C1*T4 + C2*(T3 T4) + C3*(T3 T4)*(secsza 1) + C4
   Split  : MCSST45  = C1*T4 + C2*(T4 T5) + C3*(T4 T5)*(secsza 1) + C4
   Triple : MCSST345   C1*T4 + C2*(T3-T5) + C3*(T3-T5)*(secsza-1) + C4
IV. Non linear SST
   Dual   : NLSST34    C1*T4 + C2*MCSST45*(T3-T4) + C3*(secsza-1) + C4
   Split  : NLSST45  = C1*T4 + C2*MCSST45*(T4 T5) + C3*(T4 T5)*(secsza 1) + C4
   Triple : NLSST345   C1*T4 + C2*MCSST45*(T3-T5) + C3*(secsza-1) + C4
V. PFSST  ----------------------------------------------------------------------
   T4-T5<0.7 : PFSST1   C1*T4 + C2*MCSST45*(T4-T5) + C3*(T4-T5)*(secsza-1) + C4
   T4 T5>0.7 : PFSST2 = C1*T4 + C2*MCSST45*(T4 T5) + C3*(T4 T5)*(secsza 1) + C4
--------------------------------------------------------------------------------
```

Algorithm :	C1	C2	C3	C4	RMS	Bias
SST3 :	0.332760	33.623623	0	0	5.822398	0.000421
SST4 :	1.139808	4.142020	0	0	2.192024	0.000504
SST5 :	1.114067	6.617064	0	0	3.024306	0.001120
SST34 :	1.140771	0.002094	4.220372	0	2.196253	0.000573
SST45 :	1.167966	-0.447931	4.453465	0	2.506680	0.000478
SST345 :	1.140401	0.001488	4.196631	0	2.193992	0.000567
MCSST34 :	1.003139	-0.181777	0.034983	-1.170931	1.986488	0.000503
MCSST45 :	0.994029	2.491340	0.357038	2.027301	0.948271	0.000463
MCSST345:	1.028180	0.142605	0.037031	0.439372	2.079351	0.000464
NLSST34 :	0.642803	-0.007881	-0.876466	4.377641	1.575938	0.000496
NLSST45 :	0.929538	0.079242	0.661543	3.760773	0.987222	0.000478
NLSST345:	0.644384	-0.008108	-1.095006	4.554994	1.666535	0.000521
PFSST1 :	0.996325	0.045977	2.325685	2.587247	0	0
PFSST2 :	0.915195	0.079351	0.560849	4.087021	0.979372	0.000325

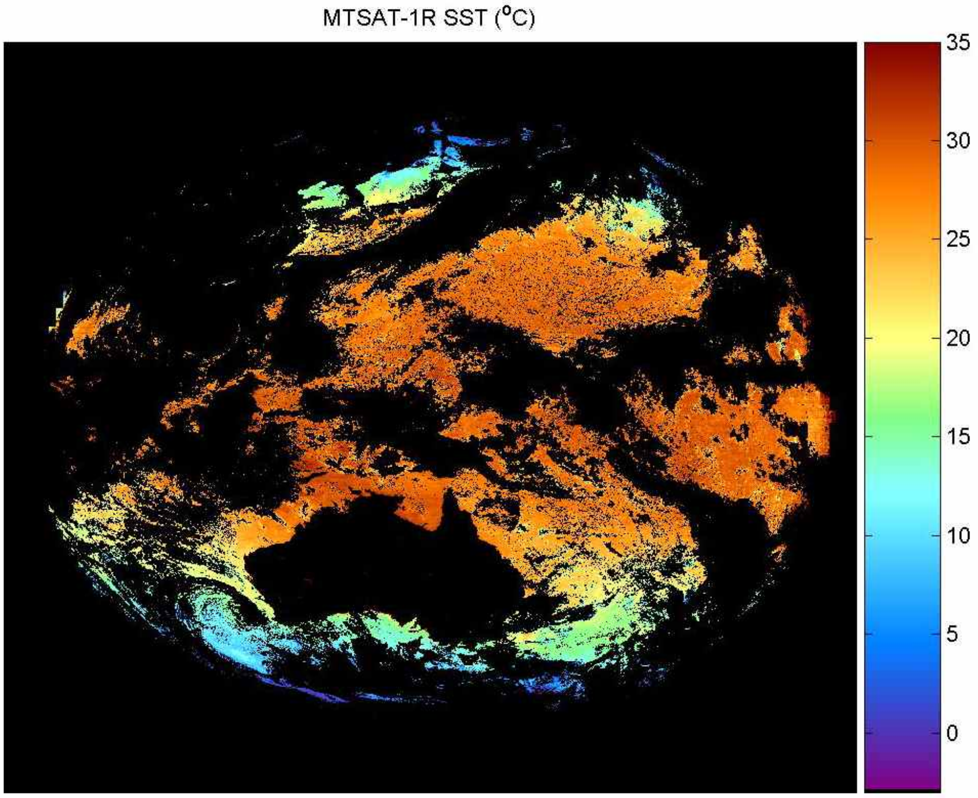

Fig. 5. An example of sea surface temperature distribution estimated from the split window MCSST equation for MTSAT-1R data (31 October 2005)

3.3.5. SST Retrieval

SST RetrievalBefore COMS launch, SST was calculated by applying MTSAT-1R Split window MCSST coefficient and formula as in (16) below to MTSAT-1R image data observed on October 31, 2005. Using the cloud detection result determined in advance for the ocean area, pixels with cloud was not calculated, but only the clear pixels without cloud were taken for the SST retrieval (Figure 6). Calculated SST field is shown in Figure 5.

$$SS \quad 1.037155\,T + 2.118685(T_4 - T_5) + 0.457718(T_4 - T_5)(\sec\theta - 1) + 1.684577 \qquad (16)$$

The coefficients shown here are ones for day time East Asian case. T4 and T5 indicate the brightness temperature of 10.8㎛ and 12.0㎛ channel in degree Celsius unit, respectively, and the θ denotes the satellite zenith angle for each corresponding pixel. Figure 6 shows visible(a) and infrared(b) images and the cloud mask result for the same time as Figure 5. Cloud contaminated pixels are still found in the retrieved SST field shown in Figure 5.

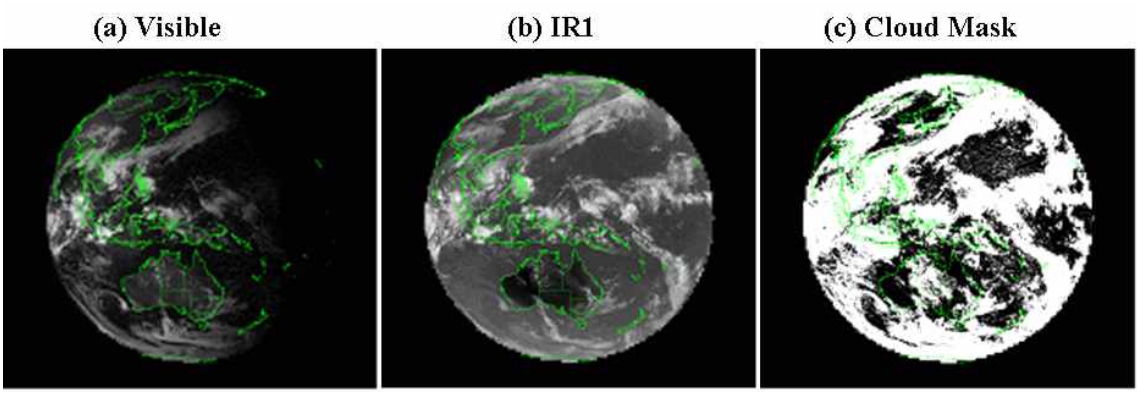

Fig. 6. (a) Visible image, (b) IR image, and (c) cloud mask image of MTSAT 1R full disk data on 31 October 2005. 3.3.6. SST Composite

3.3.6. SST Composite

When SST field is retrieved from the each observation time, large portion of the ocean can be contaminated by clouds where SST cannot be generated as shown in Figure 5. Thus, SST composite is often utilized. Both simple average and 3D-OI (3 Dimension-Optimal Interpolation) composite methods are developed in this algorithm and can be used selectively to make SST composite.

Before applying to MTSAT-1R data, composite methods are tested by using AQUA/AMSR-E day and night SST image data during the period from December 1 to 15, 2004, and both simple average and OI method are found to be working well. Figure 7 shows the example of composite SST field of each ascending and descending node from AMSR-E data from 11th ~13th of December 2003.SST is not measured on a large part depending on the observation characteristics of polar orbit satellite, such as the swath width and the orbit, other than geostationary satellite image. The example of simple average composite SST image is shown in Figure 8. Various scale vortex structures of the ocean surface can be shown well between 30 oN and 40 oN degree latitude in this SST composite image. AMSR-E SST data can be generated over broader area because they are from microwave observation, which can penetrate clouds without significant attenuation if they are not very thick or contain rainfall. However, SST was not calculated even through the composite process under convective cloud region on the ITCZ (Inter-Tropical Convergence Zone).

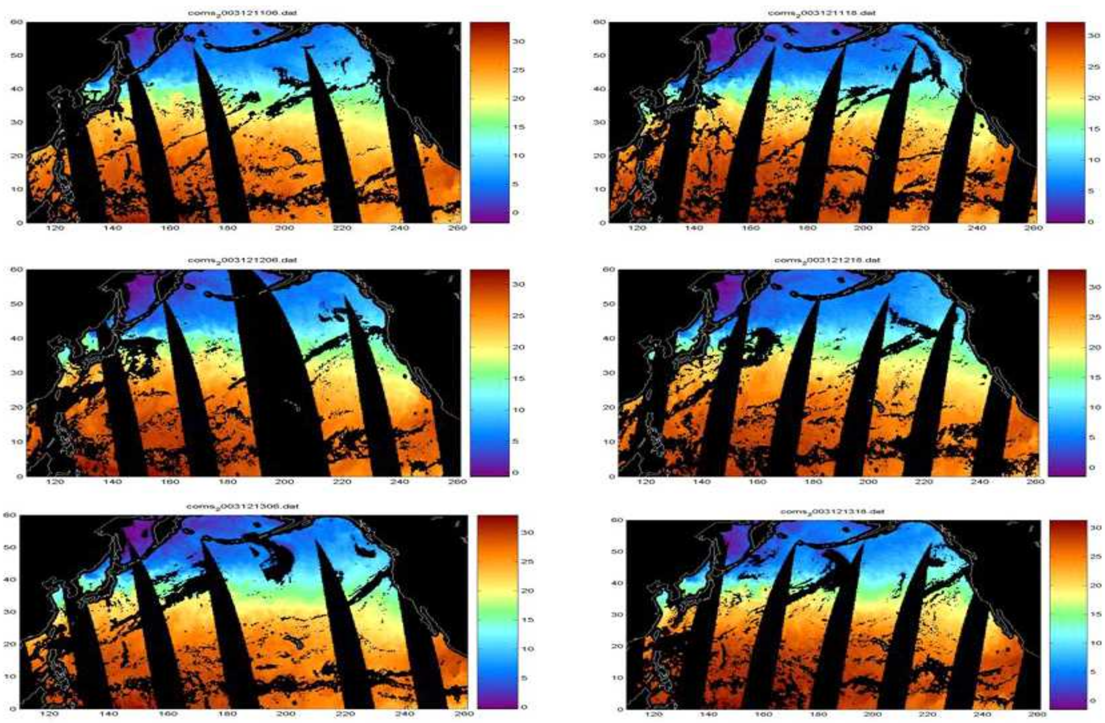

Fig. 7. Examples of SST images of AQUA/AMSR-E used for SST composite process

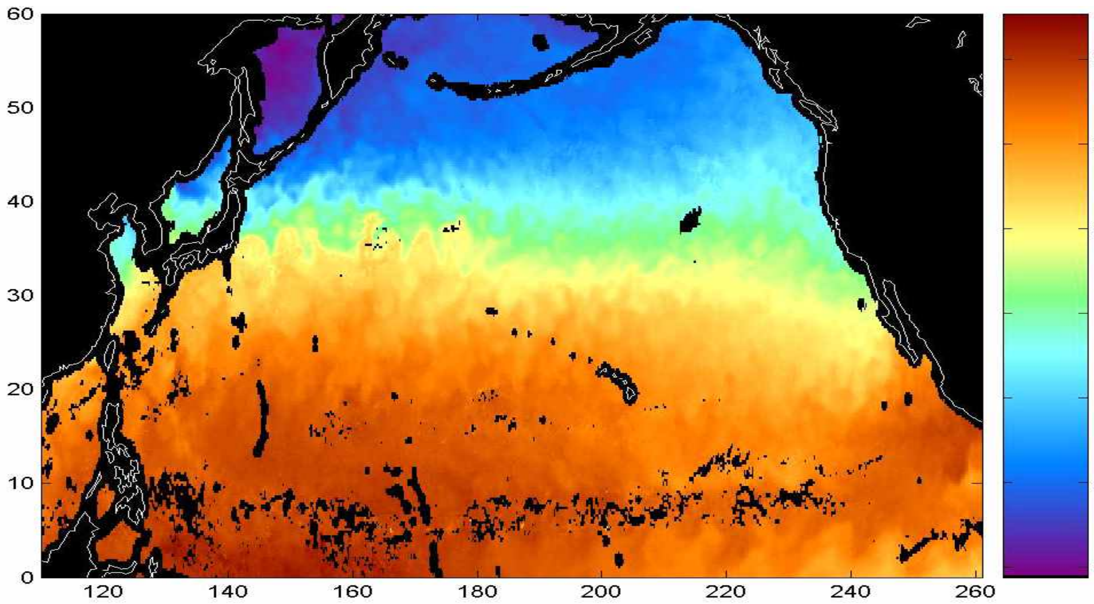

Fig. 8. An SST composite image based on simple average method

Figure 9 is the SST composite field using OI method. When OI method is used, time and space scale(Lx, Ly) for interpolation window should be given. In this experiment, Lx of 180 km and Ly of 180 km were given for east-west and south-north space scale. Moving window size was given as 8×8. This composite field is virtually made by minimizing error when there is no data. Degree of error can be calculated in each pixel and demonstrated in Figure 10. Most of pixels has the error within 0.5℃ in general, and large error over 0.4℃ is mostly found near the coast. As microwave SST is used, there is no data within 50 km range from the coast. Therefore, the large error found near the coast occurred when there is no data but calculation is made based on surrounding data. Also in some low latitude pixels, relatively large error is shown as up to 0.15℃. Except for this part, overall pacific area shows quite small error of about 0.02℃.

Comparing the composite imageries in Figure 8 and 9, OI composite field has both advantages and disadvantages. Areas with no SST data on each individual observation can be filled by objective interpolation with small error, however, vortex structures shown in simple mean field (Figure 8) become weaker and smoother. This trend depends on the spatial scale of the interpolation window applied, the smoother, the larger window is used. Size of vortex over the ocean is basically related linearly to the size of Rossby deformation radius of each ocean area. That is, this spatial scale decreases following the latitude. As the same window size was applied to low latitude and high latitude, it can reproduce the scale of actual phenomenon at latitude near equator. However, as it goes to higher latitude, a window used here is up to 10 times larger than actual phenomenon, and then detailed sea structures become disappeared. To resolve this phenomenon, window size should be given as a function of latitude and ocean area. Most institutes do not consider this issue when they make global SST composite field by OI method, and just use the same spatial scale value. Another issue with OI composite is that significant amount of computing cost is required. Considering these problems, the algorithm is structured so that the user can select from simple composite method or OI composite method in COMS composite processing. As OI method is very expensive, simple average method is utilized for the operation purpose. And 1day, 5day and 10day composite SSTs are generated as a default.

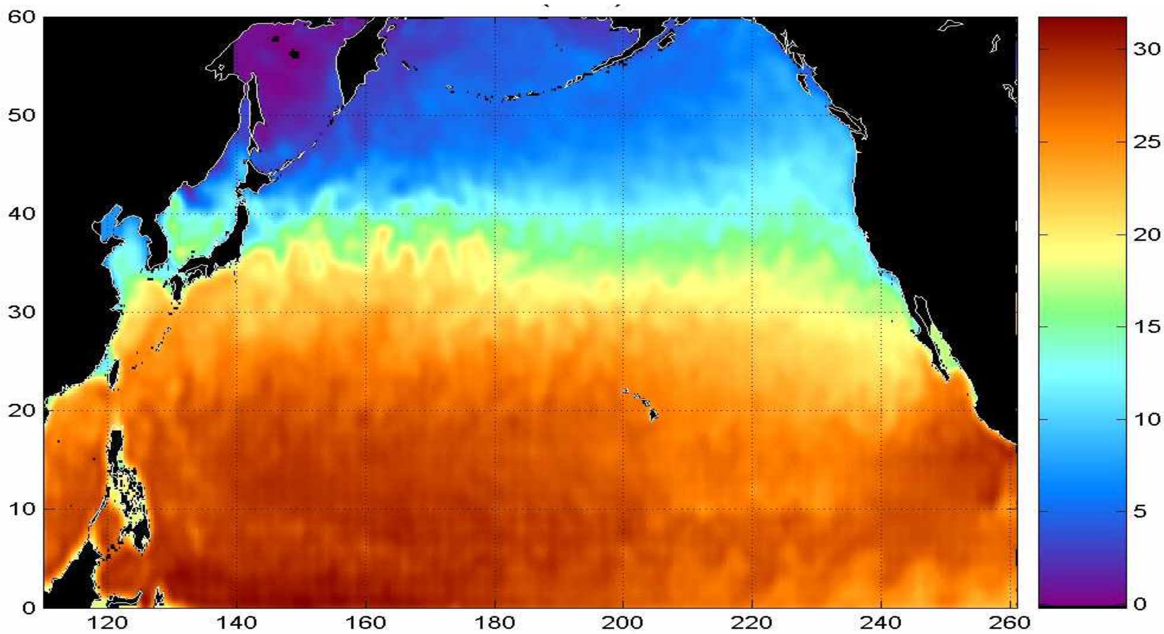

Fig. 9. SST image from OI composite technique using 8x8 window (Lx=180km, Ly=180km)

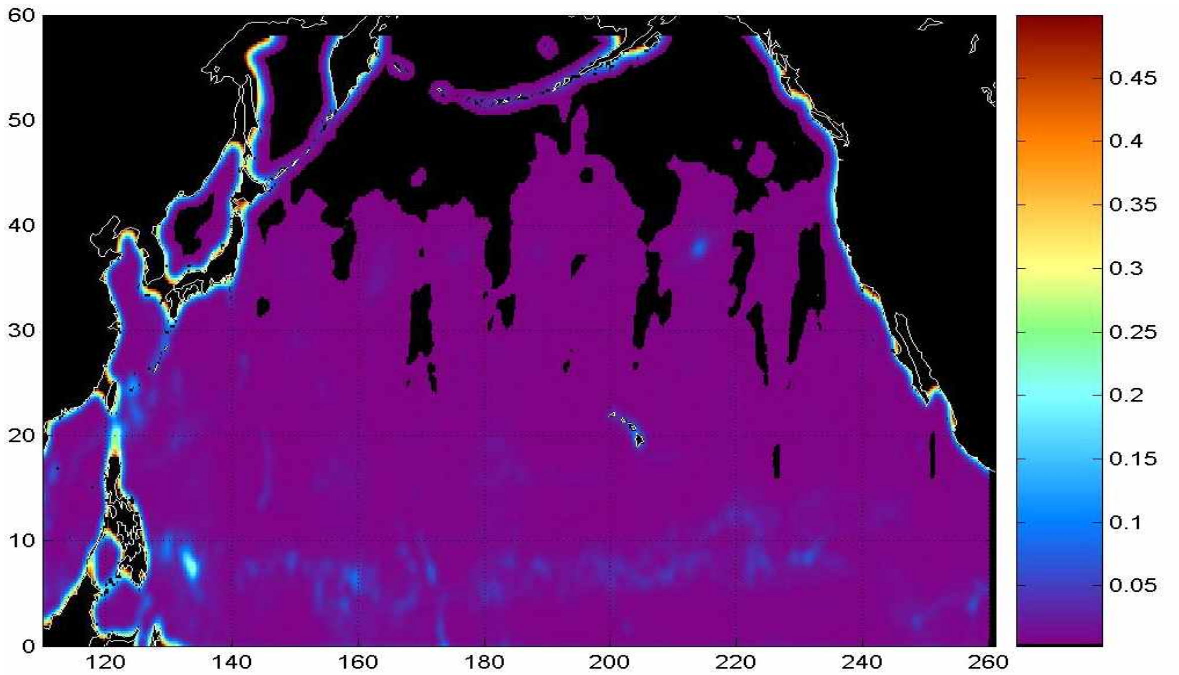

Fig. 10. An image of SST errors from OI composite technique using 8×8 window (Lx=180km, Ly=180km)

3.3.7. SST Coefficient Based on Radiation Transfer Model

As buoy-satellite match up database can be made during IOT period, COMS SST coefficients cannot be obtained before launch. So, It is required to estimate SST retrieval coefficients for COMS for the early operation phase. For this purpose, when sensor response function of each COMS channel is acquired, coefficients should be calculated in advance before IOT period. SST coefficients can be calculated using this response function, well selected rawinsonde observation data, and radiative transfer model. Sample SST coefficient was determined using MTSAT-1R channel response function. Locations of TIGR observation data are indicated in Figure 11. The color of each point represents the month of observation. Data matching COMS observation area were extracted from TIGR profiles, and 6,304 data were extracted in total.

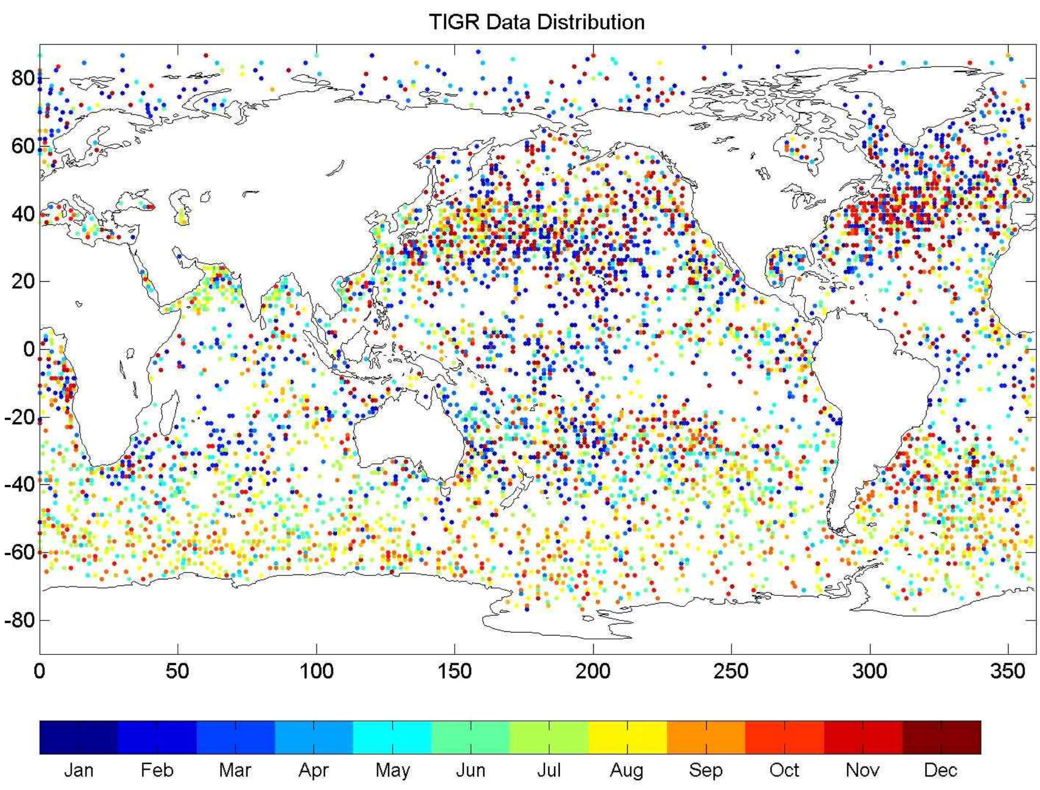

Fig. 11. Positions of TIGR data points colored according to an observation month.

With MTSAT-1R response function(shown in Figure 12) and TIGR profile data, radiative transfer model (MODTRAN 4) was used to simulate the brightness temperatures. Using those simulated brightness temperatures of 10.8㎛ and 12.0㎛, split window MCSST regression coefficients are generated. Estimated coefficients are shown in Table 8. Figure 13 shows the comparison between SSTs from TIGR data and from satellite estimation on the regression analysis for daytime(a) and nighttime(b). RMS error of calculated SST was 0.47℃ and 0.46℃ for daytime and nighttime, and bias error was 0.0349℃ and 0.0220℃, respectively.

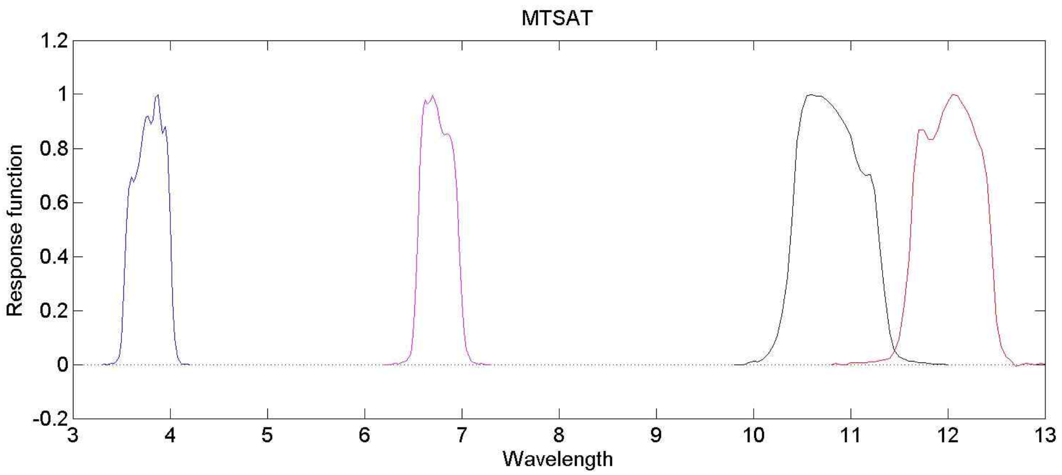

Fig. 12. Response function of MTSAT-1R channels 2, 3, 4, and 5

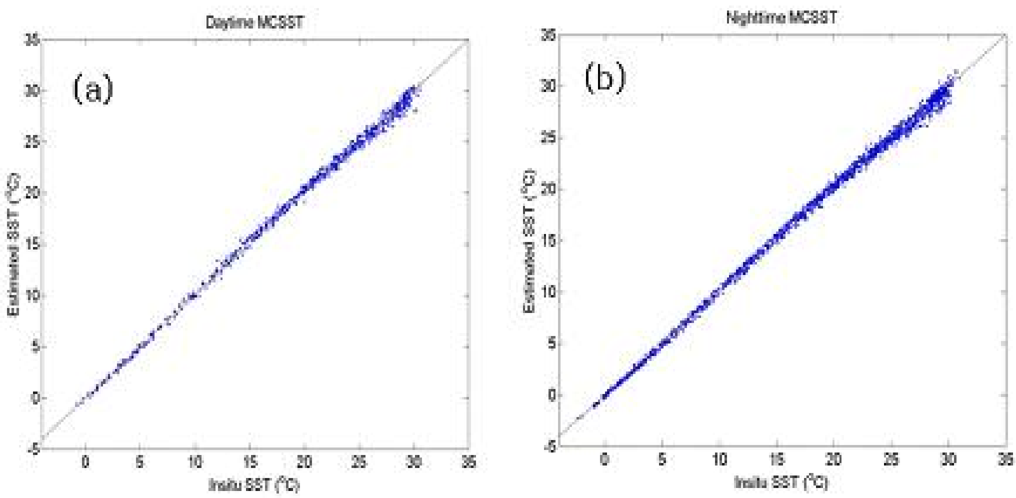

Fig. 13. Comparison of in-situ SST and (a) daytime and (b) nighttime SST estimated based on RTM and TIGR data.

Table 10. Coefficients of split window MCSST using the response function of each channel of MTSAT-1R and radiative transfer model (MODTRAN 4). SZA is satellite zenith angle.

MCSST45 = C1*T4 + C2*(T4-T5) + C3*(T4-T5)*(secSZA-1) + C4

	C1	C2	C3	C4
Day	0.9689	2.9475	0.0013	0.0356
Night	0.9690	2.9693	0.0034	0.0223

The coefficients for various SST retrieval equation employed in COMS SST algorithm are estimated from RTM simulation study using COMS channel response function for each daytime and nighttime as shown in Table 11 and Table 12, respectively.

Once COMS data is received, and the observed brightness temperatures begin to be produced, these simulated SST coefficients will be used only for the IOT period. Then they are replaced by the coefficients generated from actual observation data.

Table 11. Coefficients of daytime SST equations using the response function of each channel of COMS and radiative transfer model (MODTRAN 4). SZA is satellite zenith angle.

```
================= Daytime SST Coefficients & Regression Errors ================
I. Single channel SST without satellite zenith angle correction ----------------
          SST3=C1*T3 + C2 ,SST4=C1*T4 +C2 ,SST5=C1*T5 + C2
II. Multi-channel SST without satellite zenith angle correction ----------------
    Dual   : SST34 =C1*T4 + C2*(T3-T4) + C3
    Split  : SST45 =C1*T4 + C2*(T4-T5) + C3
    Triple : SST345=C1*T4 + C2*(T3-T5) + C3
III. Multi-channel SST with satellite zenith angle correction ------------------
    Dual   : MCSST34 =C1*T4 + C2*(T3-T4) + C3*(T3-T4)*(secsza-1) + C4
    Split  : MCSST45 =C1*T4 + C2*(T4-T5) + C3*(T4-T5)*(secsza-1) + C4
    Triple : MCSST345=C1*T4 + C2*(T3-T5) + C3*(T3-T5)*(secsza-1) + C4
IV. Non-linear SST  ------------------------------------------------------------
    Dual   : NLSST34 =C1*T4 + C2*MCSST45*(T3-T4) + C3*(secsza-1) + C4
    Split  : NLSST45 =C1*T4 + C2*MCSST45*(T4-T5) + C3*(T4-T5)*(secsza-1) + C4
    Triple : NLSST345=C1*T4 + C2*MCSST45*(T3-T5) + C3*(secsza-1) + C4
V. PFSST  ----------------------------------------------------------------------
    T4-T5<0.7 : PFSST1=C1*T4 + C2*MCSST45*(T4-T5) + C3*(T4-T5)*(secsza-1) + C4
    T4-T5>0.7 : PFSST2=C1*T4 + C2*MCSST45*(T4-T5) + C3*(T4-T5)*(secsza-1) + C4
-------------------------------------------------------------------------------
```

Algorithm :	C1	C2	C3	C4	RMS	Bias
SST3 :	0	0	0	0	0	0
SST4 :	1.244006	67.558578	0	0	2.224829	-0.001258
SST5 :	1.263684	74.969238	0	0	3.171289	-0.029487
SST34 :	0	0	0	0	0	0
SST45 :	1.280421	-0.396898	77.692726	0	2.510136	0.056822
SST345 :	0	0	0	0	0	0
MCSST34 :	0	0	0	0	0	0
MCSST45 :	0.983029	2.994210	-0.062712	-4.886696	0.469934	-0.000062
MCSST345:	0	0	0	0	0	0
NLSST34 :	0	0	0	0	0	0
NLSST45 :	0.992674	-0.012223	-0.090130	-2.478041	0.494294	-0.000062
NLSST345:	0	0	0	0	0	0
PFSST1 :	0.992556	-0.008123	-0.322725	-1.669036	0	0
PFSST2 :	1.024593	-0.012589	-0.007421	5.358628	0.446060	-0.000120

Table 12. Coefficients of nighttime SST equations using the response function of each channel of COMS and radiative transfer model (MODTRAN 4). SZA is satellite zenith angle.

```
 ================ Nighttime SST Coefficients & Regression Errors ================
I. Single channel SST without satellite zenith angle correction ----------------
   SST3 = C1*T3 + C2 , SST4 = C1*T4 +C2 , SST5 = C1*T5 + C2
II. Multi-channel SST without satellite zenith angle correction ----------------
   Dual   : SST34  = C1*T4 + C2*(T3-T4) + C3
   Split  : SST45  = C1*T4 + C2*(T4-T5) + C3
   Triple : SST345 = C1*T4 + C2*(T3-T5) + C3
III. Multi-channel SST with satellite zenith angle correction -----------------
   Dual   : MCSST34  = C1*T4 + C2*(T3-T4) + C3*(T3-T4)*(secsza-1) + C4
   Split  : MCSST45  = C1*T4 + C2*(T4-T5) + C3*(T4-T5)*(secsza-1) + C4
   Triple : MCSST345 = C1*T4 + C2*(T3-T5) + C3*(T3-T5)*(secsza-1) + C4
IV. Non-linear SST  -----------------------------------------------------------
   Dual   : NLSST34  = C1*T4 + C2*MCSST45*(T3-T4) + C3*(secsza-1) + C4
   Split  : NLSST45  = C1*T4 + C2*MCSST45*(T4-T5) + C3*(T4-T5)*(secsza-1) + C4
   Triple : NLSST345 = C1*T4 + C2*MCSST45*(T3-T5) + C3*(secsza-1) + C4
V. PFSST  ---------------------------------------------------------------------
   T4-T5<0.7 : PFSST1 = C1*T4 + C2*MCSST45*(T4-T5) + C3*(T4-T5)*(secsza-1) + C4
   T4-T5>0.7 : PFSST2 = C1*T4 + C2*MCSST45*(T4-T5) + C3*(T4-T5)*(secsza-1) + C4
-------------------------------------------------------------------------------
```

Algorithm :	C1	C2	C3	C4	RMS	Bias
SST3 :	1.068117	19.775133	0	0	0.362724	0.019607
SST4 :	1.312248	85.103638	0	0	2.208658	-0.030031
SST5 :	1.375620	103.933884	0	0	3.207777	0.006134
SST34 :	1.426230	-0.433452	115.867805	0	2.996922	0.373096
SST45 :	1.356633	-0.452766	97.211502	0	2.530137	-0.150844
SST345 :	1.395405	-0.238079	107.611496	0	2.795779	0.087616
MCSST34 :	1.018311	1.237338	-0.001922	6.542321	0.159026	0.000425
MCSST45 :	0.987531	2.987707	-0.030238	-3.705343	0.488966	0.000422
MCSST345:	1.005114	0.887679	-0.004679	2.411832	0.148573	0.000413
NLSST34 :	1.018823	-0.005025	0.029409	6.647904	0.175099	0.000418
NLSST45 :	0.996328	-0.012199	-0.043112	-1.517478	0.521346	0.000427
NLSST345:	1.009309	-0.003606	0.060947	3.420751	0.182597	0.000432
PFSST1 :	1.015329	-0.005061	0.300644	4.529645	0	0
PFSST2 :	1.033278	-0.012769	0.009341	7.492883	0.445236	0.000227

3.3.8. SST Quality Flag

SST image data is obtained only when a pixel is determined to be cloud clear. Even if cloud detection algorithm is very strict and accurate, some pixels can be contaminated by fractional cloud or thin cirrus cloud which cannot be detected easily. In this case, calculated SST field can be abnormally declined compared to the actual value. Quality flag should be given to these abnormal SST pixels to prevent the use of those pixels in next step. Various methods can be used to determine a quality flag. Either composite SST field for previous 3 days or climatological SST field can be used. For now, as there is no previous 3 days composite field, climatological SST field is set as default use for quality control in COMS SST algorithm

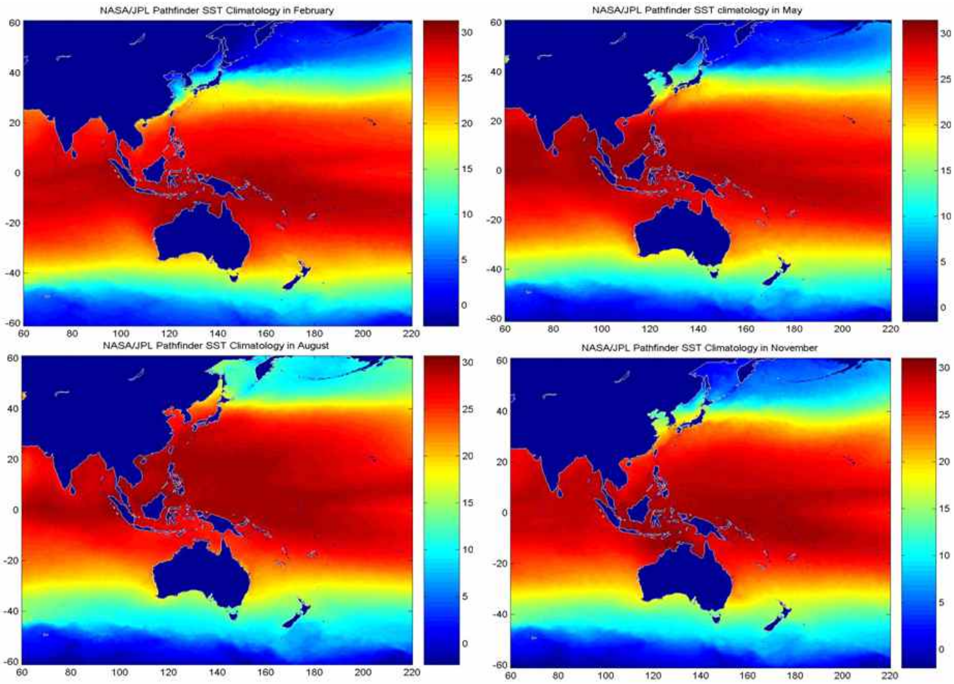

Fig. 14. Monthly sea surface temperature climatology on February, May, August, and November using 9km pathfinder SST dataset of NASA/JPL

Figure 14 shows NASA/JPL 9km resolution pathfinder monthly SST distribution. If COMS satellite observation date information isgiven, the monthly average of 2 months close to the date is found from 12 months, then it is linearly interpolated to calculate the climatology field corresponding to the satellite observation date. When the calculated SST is different from interpolated climatological value by more than 5℃, a flag is given as an abnormal value so that it is not included in SST field. Detailed flags are shown in Figure 15.

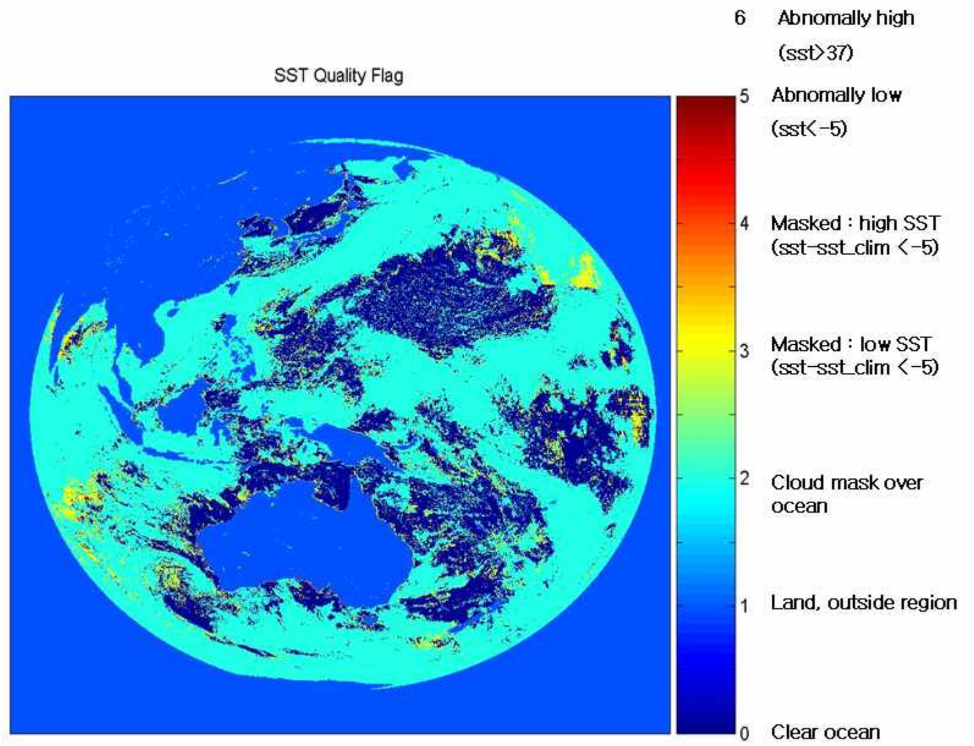

Fig. 15. SST quality flags

3.4. Validation

3.4.1. Validation Methodology

The accuracy of the retrieved SST is commonly expressed by RMSE or Bias error, compared with the conventional ocean observation data. Bias is obtained by dividing the total differences between the retrieved SST and buoy SST observation by the number of data. It represents mean bias, strictly speaking. RMSE represents the scatterness of the difference value between retrieved SST and buoy SST, and calculated from the equation (17). If the retrieval algorithm and its coefficients are well prepared, bias and RMSE will have small values.

$$an\,Bias = \frac{1}{n}\sum_{=1}^{n}(X_i - x_i) \qquad (17)$$

$$Bias = \sum_{i=1}^{n}(X_i - x_i)$$

$$SE = \frac{1}{n}\sum_{i=1}^{n}(X_i - x_i)^2$$

3.4.2. Reference Data

The first step to validate the accuracy of SST retrieval is to collect reference data. The data currently available to collect near real time is drift buoy data communicated via GTS network. However, as this data observes water temperature at a depth very close to the sea surface (~20cm) as specified in Table 13, it is a bulk water temperature but not skin temperature itself. When sea surface wind blows stronger and top layer of the ocean mixes actively, the buoy observed temperature can represent sea surface temperature, but it is not suitable in summer when solar radiation becomes stronger and seasonal thermocline is distinct. This applied to Northern subtropical ocean, and relatively large error can occur in SST field especially in summer. Most phenomena occurring due to interaction of ocean and atmosphere depend more on bulk water temperature than sea surface skin. Therefore, to reflect this water temperature in the satellite data, data corresponding to bulk of empirical regression analysis should be used. Besides drift buoy, ARGO float data, CTD observation data, and moored buoy data can be used. Because ocean data should be calibrated after observation, real time application is not easy. Therefore, active cooperation should be requested to related authorities in advance of IOT period.

Table 13. Information on available oceanic in-situ surface temperatures.

Equipment	Observation water depth	Possible data source	Remark
Drifter	15∽20cm	KMA GTS data KHOA NFRDI	
CTD	1∽5m	KHOA, NRFDI, KIOST, universities	
ARGO	3∽5m	NIMR, International ARGO Data Center, KIOST	
Mooring Buoy	1∽10m	KIOST, NRFDI, universities	

3.4.3. Temporal and Spatial Collocation

To evaluate the accuracy of SST retrieval, first, match up database on which buoy and satellite observations coincide in time and space should be made. Usually, buoy observation data includes observation time information, location (latitude, longitude), SST and observation depth, this information is used to compare with COMS satellite data to see if the satellite data is within a given time (30 minutes) and within a certain distance (5km), and to study cloud flag produced during cloud detection process to find match up point data which does not have cloud or any other problem, then series of related data are saved. In this case, for input data, brightness temperature of COMS channels (SWIR3.75㎛, IR10.8㎛, IR12.0㎛), observation location information such as latitude and longitude, and satellite time information are required. In addition, solar and satellite zenith angle, cloud and land/sea mask data are required, as well. This match up process can produce collocation data real time, provided that GTS drifter buoy data can be used on time, and it can automatically added to existing match up database. These features are equipped and match up process is considered to be performed real time in control file.

On one row, year, month, day, hour and minute of sea data observation, latitude, longitude, solar zenith angle, satellite zenith angle, maximum and minimum of channel 1, 2, 3, 4, and 5 of 3x3 pixel COMS observations, latitude and longitude of buoy data, buoy ID, buoy SST, cloud detection flag, standard deviation of channel 1 and 4 in 3 x 3 pixels, buoy observation depth, satellite retrieved SST, buoy wind direction, wind velocity and atmosphere temperature are documented in order. These data are not only used to calculate the coefficient of SST retrieval equation and but also used as basic data for accuracy and performance evaluation. The SST related module developed in this study successfully performed the function to mkae match up data and save in file.

Cloud contaminated pixels were removed from the data in which temporal and spatial collocation data was determined. Detailed process is described in Table 4 and 5 in the previous chapter, and the thresholds for quality controlwere suggested.

3.4.4. Validation Analysis

Using GTS drift buoy data and MTSAT-1R data observed in East-Asian region for one year period(July 2005 to June 2006), temporal and spatial collocation match up data was made and SST accuracy was analyzed. In the case of Split window MCSST, 0.84℃ and 0.89℃ bias scores were shown for daytime and nighttime, respectively (Figure 16). RMSE distribution for latitude rage was analized, and it is found that the region around North latitude 10-20N has low bias about 0.8℃, and the bias is amplified as it goes to higher latitude, having a value as high as over 1.2℃.

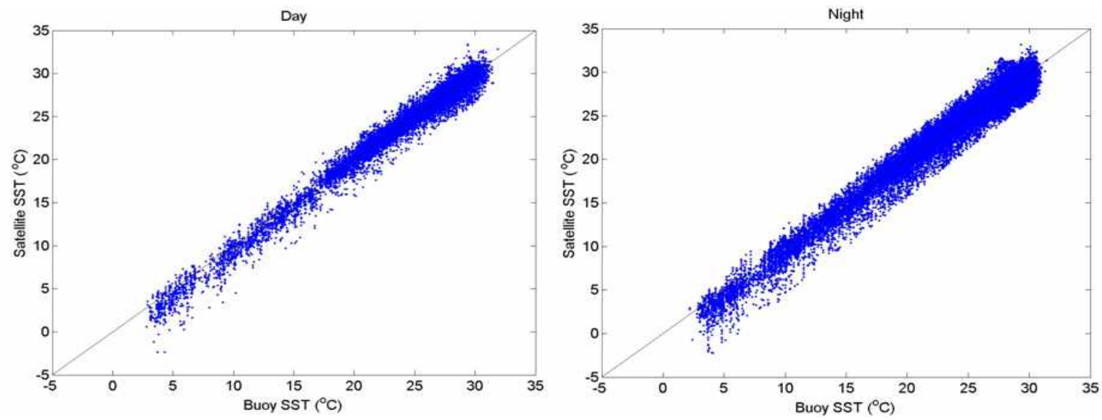

Fig. 16. Comparison of buoy SST and SST estimated from MTSAT-1R

The validation result in global domain is presented in Figure 18. Both daytime and nighttime data shows RMSE about 0.9℃.

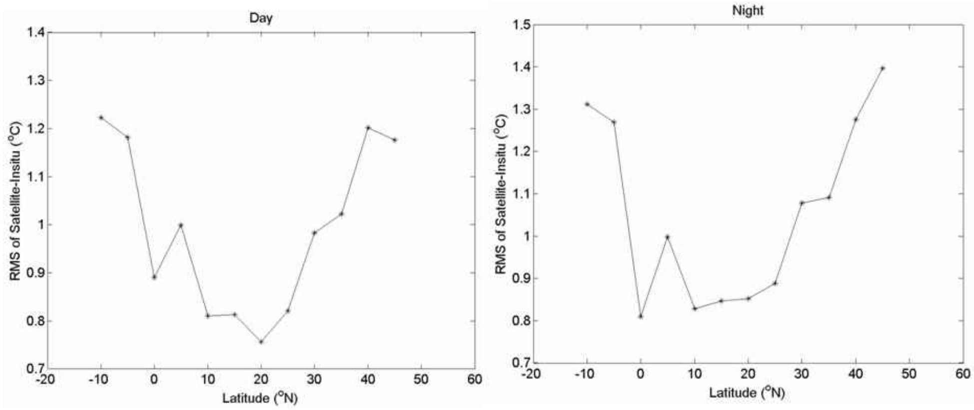

Fig. 17. Latitudinal variation of RMS errors of MTSAT-1R SST to buoy measurements

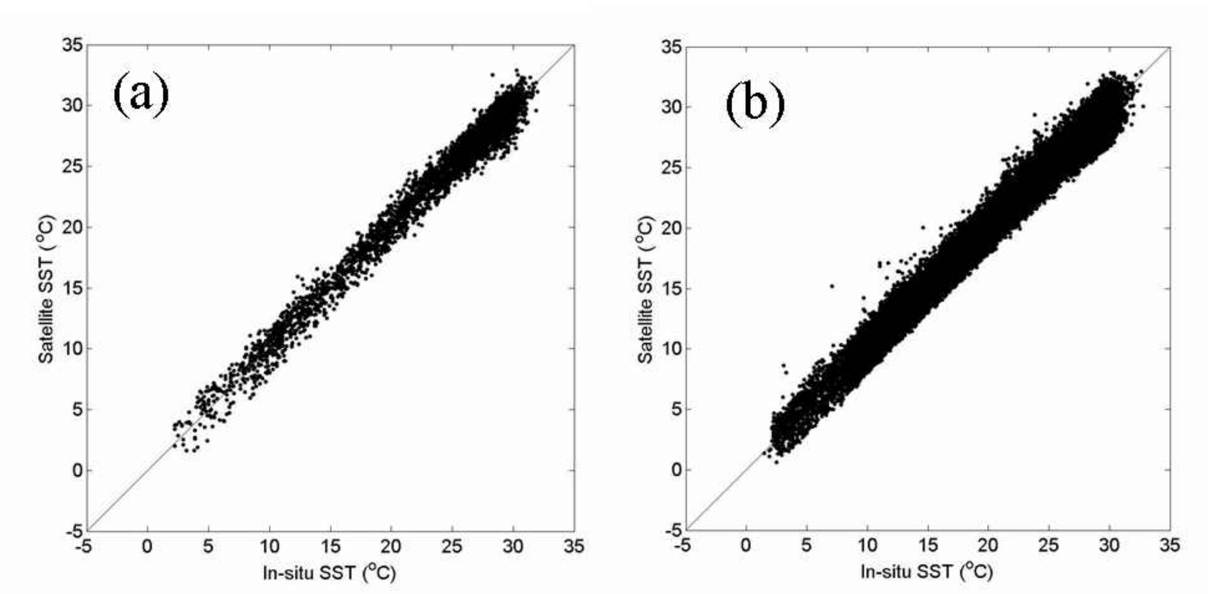

Fig. 18. Comparison of GTS buoy SST and SST estimations using (a) daytime and (b) nighttime MTSAT-1R data

4. Interpretation of Retrieval Result

Retrieved SST can be different from actual sea surface observed values due to various kinds of factors such as ocean characteristics, instrument error itself, atmospheric effect. These differences may be inevitable, however, the error sources should be understood to determine if the retrieved SST field is suitable to use. Accordingly, error characteristics of satellite-based SSTs derived from various matchup databases are analyzed.

For 5 year NOAA-14 SST in NASA/JPL, RMS error was calculated to be 1.02℃ and bias was –0.1097℃. SST of Aqua/AMSR-E which is derived using 3,118 match up data for 3 years with ARGO data showed RMS error of 0.85℃ for ascending pass and 0.71℃ for descending pass. NGSST match up database created by joint network of Northern Asian countries showed the error of 1.0℃, and SST error largely fluctuated depending on region, season and daily variation, in particular, there were more errors when wind is weak and solar radiation is high(Figure 19).

When the probability of weak wind was calculated using QuikSCAT wind data for past 6 years as shown in Figure 20, light wind frequently occurred in the area around equator, and light wind locally occurring in Western Mexico and Indian Ocean increased the temperature difference between daytime and nighttime and increased error as well. Accordingly, it should be careful to use SST field in those areas. Also in COMS area, as probability of light wind near equator is more than 80%, SST field observed by COMS satellite in daytime in summer when solar radiation is high can be calculated higher than buoy observed SST which represents bulk temperature. On the contrary, at night when stronger wind blows, vertical mixing can be activated. But when the wind is light, sea skin loses heat to atmosphere and the water temperature can be cooled remarkably lower than the bulk water temperature beneath sea skin. The calculated SST field should be carefully used according to the purpose of the user.

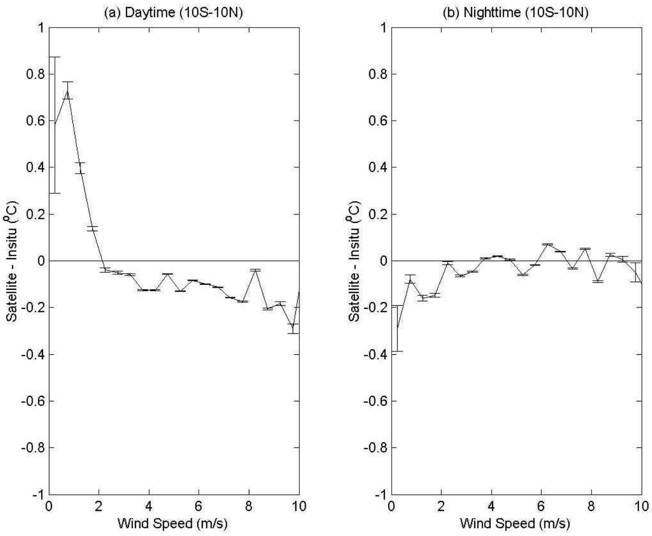

Fig. 19. SST errors as a function of wind speed at low latitude area within 10 degrees from the equator

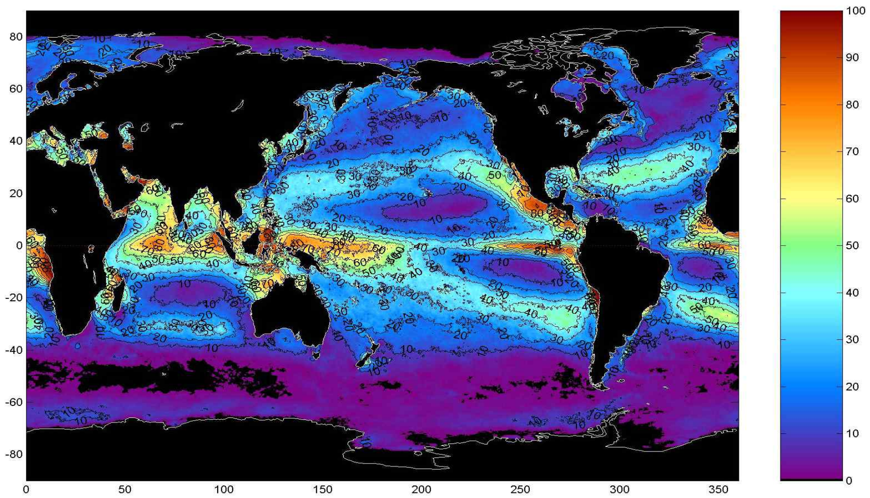

Fig. 20. Frequency probability (%) of low wind speed (<6m/s) for the period of 1999~2005

5. Post-launch tuning for COMS and Algorithm Improvement

5.1 COMS SST Coefficient Generation

COMS MCSST coefficient was determined with GTS buoy data and COMS satellite measurement data from April to June, 2011 and applied to algorithm operation(Table 14), and accuracy was improved compared to the coefficient based on RTM simulation. The buoy data used for coefficient generation and the SST estimated from that coefficients are compared in Figure 21.

Table 14. Coefficients of MCSST equations using each channel of COMS and GTS buoy data.

============== Daytime SST Coefficients & Regression Errors ==========

I. Multi−channel SST with satellite zenith angle correction

Split : MCSST45 $= C_1 * Tb_{11} + C_2 * (Tb_{11} - Tb_{12}) + C_3 * (Tb_{11} - Tb_{12}) * (\sec\theta 1) + C_4$

Algorithm :	C_1	C_2	C_3	C_4	RMS	Bias
MCSST45 :	0.985098	2.338343	0.545135	−0.321399	0.703923	0.000105

============ Nighttime SST Coefficients & Regression Errors ==========

Algorithm :	C_1	C_2	C_3	C_4	RMS	Bias
MCSST45 :	0.975640	2.496965	0.353631	-0.031189	0.735682	-0.000010

===

* T3 : COMS SWIR TBB, T4:COMS IR1 TBB, T5: COMS IR2 TBB

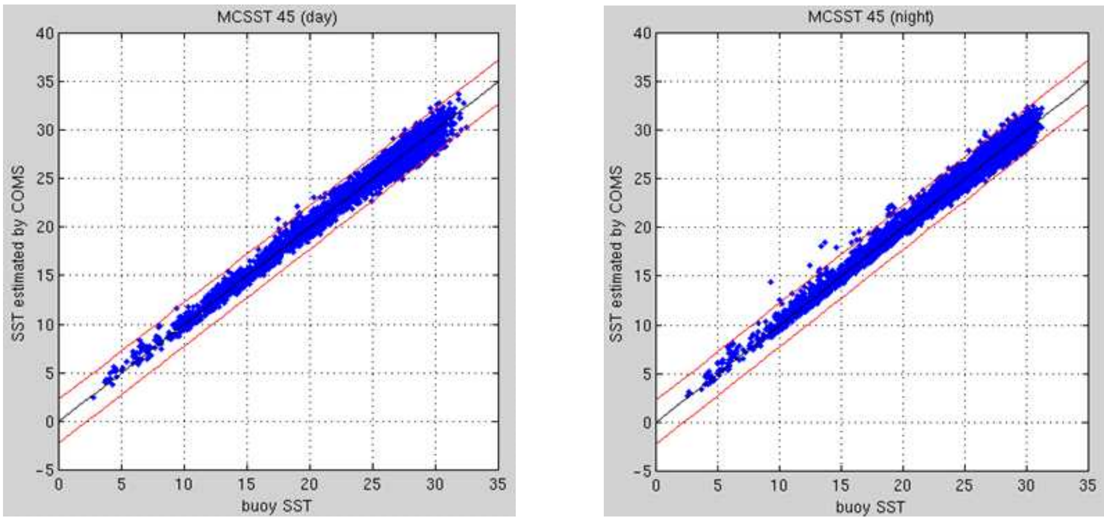

(a) (b)

Fig. 21. Comparison of GTS buoy SST and SST estimations using (a) daytime and (b) nighttime COMS data

5.2 Algorithm Improvement

To minimize the cloud contamination, which is the main cause of SST estimation error, cloud detection algorithm was reinforced. First, thin cirrus test (Figure 4; formula (16)) was applied not only to determine the coefficient but alto to calculate SST to remove cloud effect. In case when it showed large difference from climate SST value (Figure 14), it was regarded as cloud and screened out as well. Lastly, spatial uniformity test is additionally introduced for more strict cloud screening. Using the retrieved SST, when the SST at centered pixel is smaller than average SST value of surrounding 3x3 pixels and the standard deviation is larger than 1 degree, it is regarded as cloud contaminated pixel and SST are not retrieved for that pixel (set to bad value).

SST field retrieved from this algorithm and the coefficients is shown in Figure 24(b) and it shows slightly lower temperature distribution than one used RTM simulated coefficients.

5.3. Validation Result After Conversion to COMS

The results from applying new coefficients and additional cloud detection (New SST), and from applying simulated coefficients are validated comparing with the buoy data from April to June, 2011(Table 15). RMSE reduced from 2.597 to 2.037, and correlation coefficient (R) increased from 0.935 to 0.96, which show that New SST became to have better accuracy. This results showed higher values than the target accuracy of CMDPS SST, RMSE 2.247 and correlation coefficient 0.94. However, bias score showed the similar value to the target bias 1.119 degree Celsius. Compared with buoy observation, negative bias is considered to be caused mainly from an error due to incomplete cloud screening.

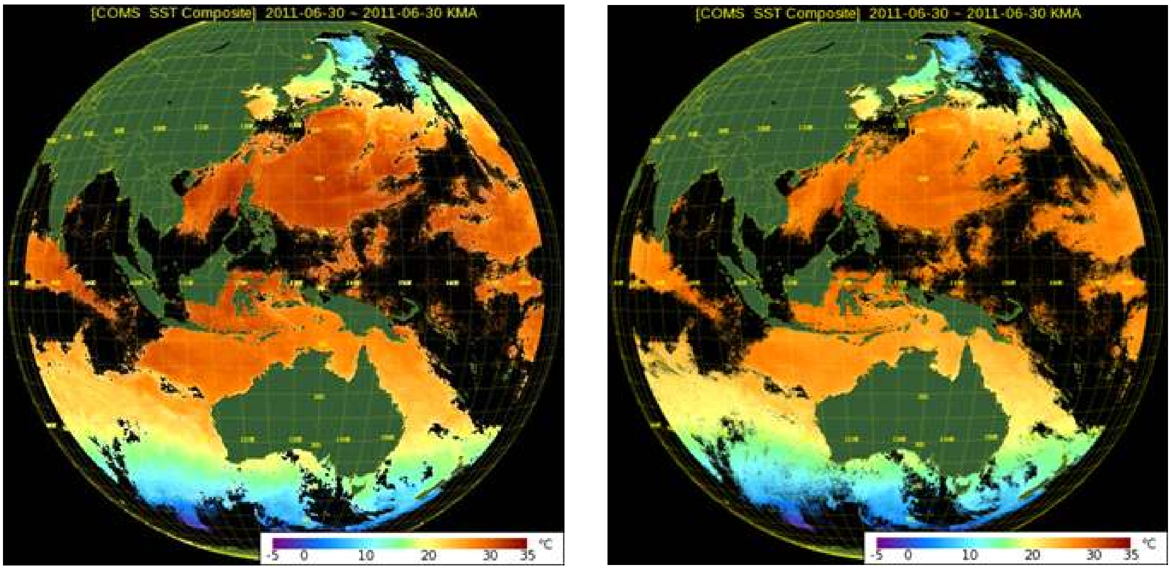

(a) (b)

Fig. 22. Comparison of SST estimations using (a) RTM based coefficients and (b) newly calculated coefficients.

Table 15. Statistical comparison between RTM based(old) and newly calculated coefficients

		RMSE	BIAS	R	N
April, 2011	OLD SST	2.757	0.730	0.920	296757
	NEW SST	1.973	-1.081	0.964	268532
	NEW SST(CN)	1.917	-1.011	0.964	225789
May, 2011	OLD SST	2.419	0.878	0.948	287883
	NEW SST	2.097	-1.219	0.963	266580
	NEW SST(CN)	2.037	-1.136	0.962	221556
June, 2011	OLD SST	2.599	1.073	0.926	307219
	NEW SST	2.038	-1.06	0.945	281300
	NEW SST(CN)	1.969	-0.965	0.933	234767
ALL	OLD SST	2.597	0.896	0.935	891859
	NEW SST	2.037	-1.119	0.96	816412
	NEW SST(CN)	1.974	-1.036	0.959	682112
	Target value	2.247	-1.052	0.94	

6. Considerations and Further Improvement

In current SST retrieval process, firstly collocation data between real ocean observation data and COMS satellite data is produced, and SST coefficients are generated through empirical regression analysis. The most important process is collecting accurate and large amount of ocean observation data. Currently, a lot of data such as drifter buoy SST data acquired from KMA GTS network are being used, but, in order to characterize the bulk sea surface temperature well enough, SST data observed froum various sources are needed to use. CTD data are available from KHOA (Korea Hydrographic and Oceanographic Administration), NFRDI (National Fisheries Research and Development Institute), research institutes, and universities. KHOA is floating a significant number of drifters on the sea to observe costal stationary water temperature, and operates mooring buoys and ARGO floats. These data can be used only after precise adjustment process. Therefore, close cooperation and effort are required to secure these data before launching COMS.

Maintaining observation instruments in a constant depth is not easy. Drift buoys are operated around 20cm below the ocean surface. They are apt to be in a constant depth when ocean condition is calm. But, when vertical motion caused from wave or wind is active, it is hard to maintain a constant depth. For CTD data, temperatures measured at a few meters below the surfaceare normally used, discarding observed temperature at nearer ocean surface at data adjustment stage. Therefore, these different observation at different depths of each instrument can attribute to the SST retrieval error.

The diurnal change of vertical temperature structure is another main error source.

The examples of vertical structure change of water temperature at nighttime and daytime are presented in Figure 23. During the daytime, the water temperature in the ocean surface boundary layer observed by satellites is the highest, and the temperature rapidly decrease as it goes deeper, reaching a certain water depth to the mixed layer as shown in Figure 23a. In the contrary at nighttime, as sea surface cools down and has the lowest water temperature, water temperature increases as it goes deeper in the sea(Figure 23b). However, the vertical structure of water temperature near sea surface does not necessarily follow Figure 23 all the time. When wind blows stronger during the day, ocean boundary layer is actively mixed and can lose heat to the atmosphere, providing lower water temperature on the ocean boundary layer. At night, horizontal advection of warm atmosphere can locally heat the sea skin, providing higher water temperature than surface layer.

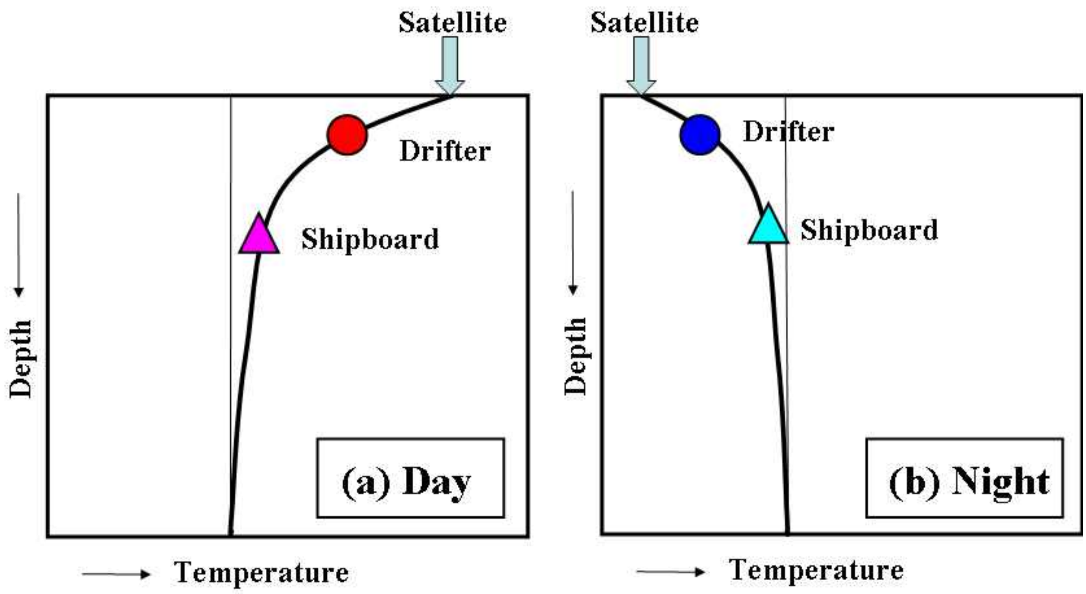

Fig. 23. Schematic plots of vertical temperature profiles of the layer within a few meters from the sea surface according to daytime and nighttime. Oceanic instruments of satellite-tracked surface drifting buoy and CTD measures sea surface temperatures at different depth

Water temperature at ocean boundary layer can have up to 2.5℃ of difference between daytime and nighttime. The infrared image data used in this study observes radiation energy coming from within some μm from the sea surface. But, as it is calculated as SST through the coefficients empirically analyzed in regression between 20cm and 5m water depth, it is not SST of some μm, nor sea skin water temperature, strictly speaking. Satellite SST is shown to be more similar to sea skin buoy temperature rather than CTD observation by sea survey ship, and it showed a large difference from CTD water temperature by up to ±3℃. When SST coefficients are induced for ocean, water temperature observed by CTD or mooring buoy should pass adjustment process, so it can be acquired later in time. As buoy data can be obtained almost real time, it is used the most to generate SST coefficients. It infers that the more the buoy observation data, the more change of water temperature by buoy can be reflected by induced coefficients. Water temperature on the ocean boundary layer can change more easily with strong mix of turbulent flow by wind rather than the molecular diffusion between ocean-atmosphere. Therefore, even though the temperature on ocean boundary layer is important, knowing the water temperature on the surface layer beneath the sea surface enables better understanding of marine phenomena, and more proper use as input data of ocean circulation model and climate-weather forecast model. Therefore, more field observation on the vertical structure of sea surface layer temperature should be made, and understanding of local characteristics of SST errors should procede. To see the diurnal variation of SST, time series image data of SST in summer with large solar radiation was analyzed. Infrared sensor data like AVHRR is more likely to fail to detect cloud at night when visible channel data is not available. Area contaminated by cloud produces significantly low SST than surroundings, so daily variation of SST can be amplified by the failure of cloud detection at SST calculation, rather than being actual ocean phenomenon. Therefore, SST data of AQUA/AMSR-E microwave sensor available without being absorbed by cloud, was used. Data period was set to be one month of August 2002.

Fig. 24a and 24b show mean SST distribution of ascending pass for day and descending pass for night. Mean water temperature field, difference of SST between day/night (Figure 21c), and maximum day/night water temperature difference of each pixel (Figure 24d) were determined from formula (18) and (19).

$$ST_{,j} \quad \frac{1}{L_{,j}} \sum_{k=1}^{L_{i,j}} SST_{A_{i,j,k}} \qquad (18)$$

$$SST_{D_{i,j}} = \frac{1}{M_{i,j}} \sum_{k=1}^{M_{i,j}} SST_{D_{i,j,k}}$$

$$\triangle SST_{i,j} = \frac{1}{N_{i,j}} \sum_{k=1}^{N_{i,j}} (SST_{A_{i,j,k}} - SST_{D_{i,j,k}})$$

$$\triangle SST_{i,j} = SST_{A_{i,j}} - SST_{D_{i,j}}$$

$$\triangle SST_{\max_{i,j}} = sst_{i,j} | sst_{i,j} \equiv Max(\triangle SST_{i,j,1}, \triangle SST_{i,j,2}, \cdots, \triangle SST_{i,k,N_{i,j}}$$

(19)

Here, $SST_{A_{i,j}}$ and $SST_{D_{i,j}}$ are SST at daytime and nighttime observed at the latitude and longitude of a random pixel, i, j. $L_{i,j}$, $M_{i,j}$ indicate the number of SST observed from each pixel at daytime and nighttime for the whole data period.

$,j$ indicates the number of SST data of the location on which SST is observed at both daytime and nighttime. Even when microwave sensor is used, SST data cannot be measured if strong rainfall or vertical cloud is developed, thus, the number of SST data is expressed as a function of location $,j$ at all pixels. Mean distribution of day/night water temperature difference was obtained by first determining daily SST difference at day and night for all pixels and then determining the mean.

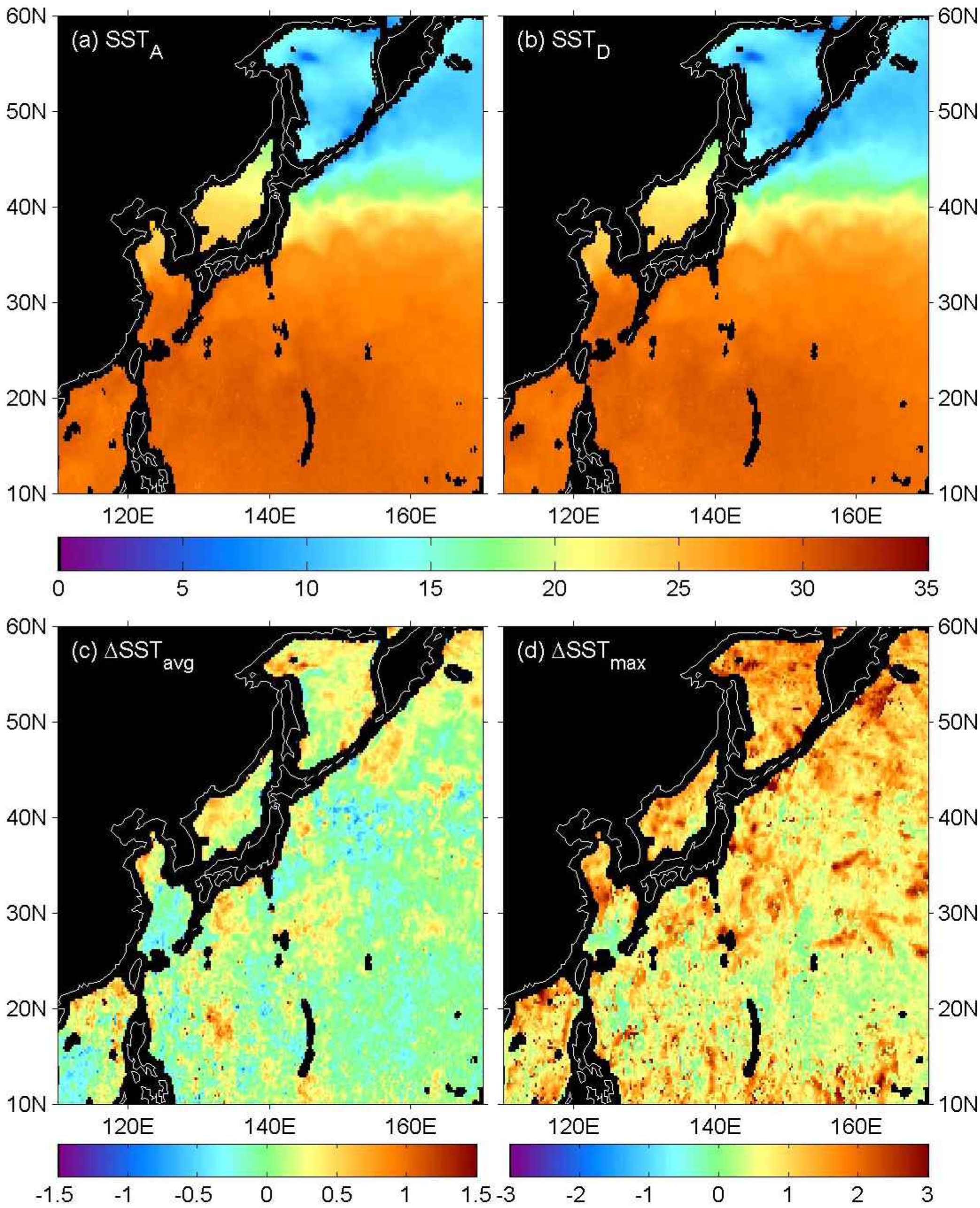

Fig. 24. Sea surface temperature averaged for (a) daytime ascending passes and (b) nighttime descending passes of AQUA/AMSR-E in August, 2002. (c) is the average map of SST difference between daytime and nighttime SST for the same day and (d) shows the maximum of diurnal difference of each day for a month of August in 2002

In spring or fall like in April or November, vertical stratification of sea water is smaller than summer, leading smaller daily temperature variation. Therefore, August was selected because daily SST variation is the largest, and SST mean field of day and night using the data for a month of August 2002 is shown in Figure 24a and 24b. It is not easy to discern SST difference by bare eye. In Figure 24c, daily SST variation is determined and the mean for the whole period is shown on each pixel. Negative values are found in East of Japan, where Kuroshio current flows, East China Sea north of Taiwan, and low latitude ocean area between 10°N and 20°N. Overall, positive values up to 1.5℃ are widely distributed. In the case of East Sea, North West of the East Sea showed larger daily variation range of SST than South Eastern part. As daily temperature variation was averaged by time in Figure 24c, actually daily variation may not be significant phenomenon. Accordingly, the maximum day SST difference for the month was found and presented in Figure 24d. For maximum for a month, over 98% of pixels showed positive value, and in over 42%, water temperature during the day was much higher than night by over 1℃ . The daily difference of SST was reported to be normally larger when wind is light and solar radiation inflow is high, and stratification is well developed (Donlon et al., 2002). Daily difference of SST greatly affects change of ocean-atmosphere interaction. Cornillon and Strammer(1985) pointed out that if daily variation of SST is included in calculation of monthly SST field, water temperature increases by 0.2℃ which corresponds to 5Wm^{-2} of heat flux. In the case of NOAA/AVHRR, daily variation reached as high as 6.6℃(Flament et al., 1994). These problems suggest that more observation is required to figure out the vertical structure of the sea. It is expected that if water temperature between 0~3 m can be constantly observed, a technology to reprocess the SST field assimilated in numeric forecast model can be developed.

Cloud is the largest obstacle in SST . If cloud detection is not perfect, most SSTs are calculated low. These values are to be removed by comparing with climate data or previous composite field. However, this approach may not be appropriate in area that has large even in the same period. and fluctuation of each area should be understood so that the same threshold is not given to SST flag but it can change according to localcharacteristics.

If day and night are present in one image, current algorithm either day or night . It was to prevent discontinuous boundary of SST field that occurs when different algorithm is used in one image. When this discontinuous boundary is directly used as input field of the numeric model, it acts like a large thermal front by changing the stability of sea-atmosphere boundary layer. Change of stability and spatial difference produce phenomena due to -atmosphere interaction in the model. The accuracy of prediction by model varies depending on input data, and the result of the model can go in an unpredictable . up database should be continuously produced and and characteristics of the error should be understood and coped with. These characteristics can be figured out if real time match up process is made between MTSAT-1R data and data and large number of match up database is produced.

7. References

Bernstein R. L., 1982, Sea surface temperature estimation using the NOAA-6 satellite Advanced Very High Resolution Radiometer, J. Geophys. Res., 87, C12, 9455-9465.

Barton I. J., 1985, Transmission model and ground-truth investigation of satellite-derived sea surface temperatures, J. Clim. Appl. Meteorol., 24, 508-516.

Donlon, C. J., T. J. Nightingale, T. Sheasby, J. Turner, I. S. Robinson, and W. J. Emery, 1999. Implications of the oceanic thermal skin temperature deviation at high wind speed. *Geophysical Research Letters*, 26(16): 2505-2508.

Donlon, C. J., P.J. Minnett, C. Gentemann, T. J. Nightingale, I. J. Barton, B. Ward and M. J. Murray, 2002. Toward improved validation of satellite sea surface skin temperature measurements for climate research, *J. Climate*, 15: 353-369.

Flament, P., J. Firing, M. Sawyer and C. Trefois, 1994. Amplitude and horizontal structure of a large diurnal sea surface warming event during the Coastal Ocean Dynamics Experiment. *J. Phys. Oceanogr.*, 24: 124-139.

McClain E.P., Pichel W.G. and Walton C .C., 1985, Comparative performance of AVHRR-based multichannel sea surface temperature. J. Geophy. Res., 90, 3655-3661.

McMillin, L. M., 1975, Esimation of sea surface temperatures from two infrared window measurements with different absorption, J. Geophy. Res., 80, 5113-5117.

Prabakahara C., Dalu G. and Kunde V.G., 1974, Estimation of sea surface temperature from remote sensing in the 11 - 13 μm window region, J. Geophy. Res., 79, 5039-5044.

Walton, C.C., 1988, Nonlinear multichannel algorithms for estimating sea surface temperature with AVHRR satellite data. J. Applied Meteor., 27, 115-124.

Walton, C.C., W.G. Pichel, J.F. Sapper, and D.A. May, 1998, The development and operational application of nonlinear algorithmss for the measurement of sea surface temperatures with NOAA polar-orbiting environment satellites, J. Geophy. Res., 103, C12, 27999-28012.